

Radar and AI-based Soil Moisture Monitoring for Efficient Farm Irrigation

A Major Qualifying Project (MQP) Report Submitted to the Faculty of
WORCESTER POLYTECHNIC INSTITUTE in partial fulfillment of the requirements for the
Degree of Bachelor of Science in Computer Science

By:

Allen Cheung

Ruba Khan

Project Advisors:

Seyed Zekavat

Oren Mangoubi

Doug Petkie

Date: May 2024

This report represents work of WPI undergraduate students submitted to the faculty as evidence of a degree requirement. WPI routinely publishes these reports on its website without editorial or peer review. For more information about the projects program at WPI, see [http:// www.wpi.edu/](http://www.wpi.edu/)

Academics/ Projects.

Abstract

This study presents a novel approach using Stepped Frequency Continuous Wave (SFCW) radar technology and machine learning models to develop a non-invasive, cost-effective method for soil moisture estimation. Using the Akela AVMU radar system, we collected and processed radar data, which was then combined with ground truth data moisture data collected using the PR2-Probe by Delta- T Devices. Various machine learning models were applied to data the, with Gradient Boosting Regressor achieving the best overall model performance with a test RMSE of 0.408 when predicting soil moisture at the depth of 20 cm and XGBoost Regressor achieving a test RMSE of 0.814 which is the best overall for the depths of 0 to 40 cm combined. Despite challenges like extended model run times, complex data handling, and limited data size, our study achieved significant improvements in non-invasive soil moisture prediction methods. This research helps open avenues for broader applications in agriculture such as ground water level assessment and drought prediction, contributing to sustainable agricultural practices.

Acknowledgements

We would like to thank everyone for their involvement in this project. Their help led us to successfully complete our MQP.

1. USDA
2. Michigan Tech Research Institute (MTRI)
3. Brian Wilson, MTRI
4. Himan Namdari, WPI
5. Vincent Filardi, WPI

Table of Contents

Contents

Abstract	ii
Acknowledgements	iii
Table of Contents	iv
Introduction	1
Project Objectives	1
Task 1: Data Collection	2
Task 2: Probe Data Analysis	2
Task 3: Understand SFCW and Extract Information	2
Task 4: Dataset Creation	2
Task: 5 Machine Learning	2
Background	3
Data Collection and Experimental Setup	5
Site Setup	5
Radar System Configuration	5
Antenna Setup	6
Moisture Probe	7
Data Collection Methodology	7
Data Processing and Analysis	8
Probe Data Analysis	9
Descriptive Statistics Overview	9
Correlation Analysis	11
Moisture Distribution Analysis	12
Understanding the SFCW Radar	14
Dataset description	16
Machine Learning	18
Experimental Results	19
Conclusion and Future Work	22

Bibliography	25
Appendix A	28
Appendix B	37

Introduction

Accurate soil moisture estimation and measurement is important for optimal irrigation, crop yields, and soil health. Soil moisture estimation not only allows for efficient usage of water, but also supports sustainable practices [1]. Recently, ground-penetrating radar (GPR) has shown promise for soil moisture and characteristics measurements due to its non-invasive methods to collect data over a large area [2]. However, the setup, radar configuration, and the environment introduce noise and interference to the GPR data. Therefore, it is important to take account of them in the GPR data analysis process.



Figure 1: Image depicting an SFCW radar over a mega farm creating soil moisture maps.

Project Objectives

This study aims to develop and implement a machine learning-based model to analyze soil moisture data collected using a Stepped Frequency Continuous Wave (SFCW) radar called AKELA AVMU. Through the combination of radar technology and machine learning models,

we aim to provide a cost-friendly, non-invasive, and high-resolution method to estimate soil moisture to enable more sustainable water resource usage.

Task 1: Data Collection

To develop a method for collecting soil moisture radar data using the AKELA AVMU radar system and ground truth soil moisture data using the Delta-T Devices PR2 Profile Probe while also maintaining accurate and efficient data collection.

Task 2: Probe Data Analysis

Analyze the collected ground truth soil moisture data.

Task 3: Understand SFCW and Extract Information

Gain an understanding of the SFCW radar technology and extract relevant information from the soil moisture radar data, such as raw/complex values, magnitude, and phase.

Task 4: Dataset Creation

Create a dataset that contains the processed radar data and ground truth soil moisture data while making sure it is organized and ready for machine learning applications.

Task: 5 Machine Learning

Run and evaluate different machine learning models (Linear Regression, Random Forest, Gradient Boost Regression, Support Vector Regressor, Multi-layer Perceptron, etc) to identify the most efficient and accurate model for estimating soil moisture at different depths, different datasets, and different radar data subsets.

Background

The one key element in agriculture, environmental monitoring, geology, and many others is soil moisture and being able to monitor it allows stakeholders like farmers to make well informed irrigation decisions to improve water management. Some methods of measuring soil moisture range from satellite imagery to soil sampling and for many reasons, they are limited. Examples include, low-resolution imaging, lack of depth penetration, invasive, and cost [3]. This study aims to overcome these challenges.

As humans increase agricultural productivity, water tends to become scarce and comes the need for efficient and accurate estimation of soil moisture. As stated before, many of the current methodologies have drawbacks: satellite imagery lacks resolution and does not reach the root zone, probing the soil is invasive, expensive, and does not scale well [4]. Advances in the field of subsurface sensing demonstrate the power of GPR. The SFCW radar stands out due to its high resolution and ability to penetrate many subsurface materials [5].

There are still many challenges when estimating soil moisture using a SFCW even if radar technology has become more advanced. The data received is usually in-phase and quadrature elements and needs to be processed. In addition, data handling and analysis is more complex due to manual collection of data and data being disorganized. We evaluate several machine learning models using RMSE and through the transformation of radar values into different attributes (raw/complex (real and imaginary), magnitude, and phase) to set new benchmarks in the field of soil moisture estimation and GPR data analysis.

Collaborating with the Michigan Tech Research Institute (MTRI) and Worcester Polytechnic Institute (WPI), we capture data from realistic agricultural settings to improve the accuracy of soil moisture estimation.

Data Collection and Experimental Setup

Site Setup

To conduct our experiments, we chose a plot of land at 87 Prescott St in Worcester, Massachusetts. Since the native soil in the area contained large, hard rocks, we excavated the site so that these rocks would not present themselves as an interference in our measurements. The soil was replaced with a uniformly compacted layer of loam to mimic long-term farmland soil conditions. This site was then left to settle naturally for several days after the compaction process to stabilize the structure, thereby minimizing any potential discrepancies in data due to soil instability.

Radar System Configuration

Our study utilized the Akela AVMU radar which is a version of the Stepped Frequency Continuous Wave (SFCW) radar system renowned for its precise and dependable data collection capabilities. The radar was set to operate over a frequency range of 400 MHz to 2 GHz, a common spectrum in GPR applications due to its optimal balance between depth penetration and resolution. The frequency response of the site was measured by stepping the transmitter through each frequency incrementally, allowing the radar to capture echoes from the scene and mix them with the transmitted signal to compute complex values indicative of the subsurface characteristics. This configuration provided an estimated penetration depth of up to 400 meters in a vacuum and was optimal for our setup.

Antenna Setup

Two types of antennas were employed: the Log Periodic (LP) Antenna [6] and the Vivaldi Antenna [7] as seen in *Figure 2A* and *Figure 2B*. The LP antenna is known for its broad frequency bandwidth and consistent radiation pattern. The Vivaldi antenna is characterized by its planar look with a tapered slot and offers ultra-wide band frequency coverage and high gain. This structure makes it suitable for multiple operational frequencies with minimal signal loss.



Figure 2: Log periodic antenna (co-pole) and ladder structure (Fig. A), Vivaldi antenna (cross-pole) wooden structure(Fig. B),
Customized wooden structure with three heights h_1, h_2, h_3 (Fig. C)

Moisture Probe

For ground truth data collection, the Probe-PR2 and HH2 moisture meter from Delta-T Devices were used. These instruments were used to measure soil moisture at 10 cm, 20 cm, 30 cm, and 40 cm below ground, allowing for a comprehensive profile of the soil's moisture content across different layers. Data from these probes were collected at six positions namely A1, A2, B1, B2, C1, and C2. The measurements of these were then averaged to come up with one reading for each position A, B, and C.

Data Collection Methodology

To ensure comprehensive soil analysis, radar data was collected at various heights of 35 in, 54 in, and 79 in above ground as seen in *Figure 2C*. All measurements were conducted every 2 hours to ensure that any changes in soil moisture were accounted for. For each measurement round, radar data was collected above point A, point B, and point C and to simulate drone movements, radar data was collected in a sweeping motion moving from point A to C as seen in *Figure 3*. This series of collections was done of each of the heights and each of the antenna types as well. Each measurement point was sampled 100 times to ensure data reliability. After radar data was collected, moisture data, along with external temperature, soil temperature and UV index was also recorded.

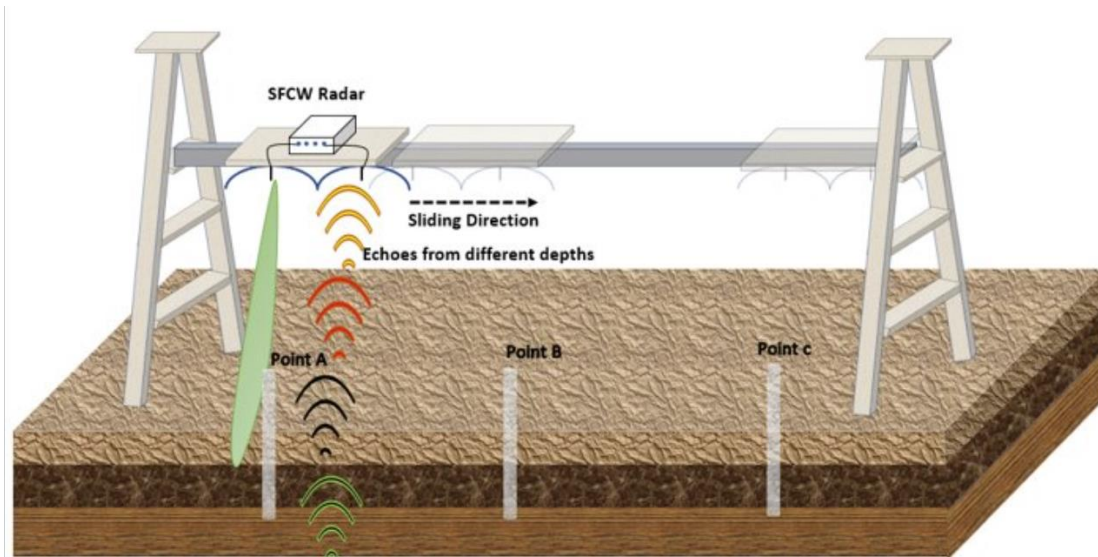


Figure 3: Experimental setup demonstrating each probe and the different positions of the radar

Data Processing and Analysis

The data recorded by the radar system in a .imb format contained amplitude, phase, and complex value information processed using AKELA APRD software and MATLAB. This analysis included the generation of range and delay profiles and an evaluation of signal attenuation across different frequencies, providing insights into the subsurface conditions.

Probe Data Analysis

In this section, we present the analysis of the data gathered from moisture probes inserted at depths of 10 cm, 20 cm, 30 cm, and 40 cm, across various points and times within our test site. The aim is to understand the statistical characteristics of soil moisture, examining the correlation, distribution, and variability across different depths to better understand the soil moisture dynamics.

Descriptive Statistics Overview

Our dataset comprises 153 measurements of each depth, reflecting a robust set of data points that show a detailed examination of soil moisture trends. The average moisture content shows a gradual increase with depth, with values starting at 25.05% at 10cm and rising to 40.24% at 40cm as seen in *Table 1*. This increment suggests a trend of moisture accumulation at deeper soil layers. The standard deviation indicates variability in measurements, which is relatively high at 30 cm, suggesting fluctuating moisture levels possibly influenced by external environmental factors or soil heterogeneity. The range of measurements, marked by the minimum and maximum values, highlight the moisture extremes with particularly notable fluctuations observed at the deepest layer of 40 cm. These fluctuations could be attributed to underlying water tables or distinct soil properties that affect moisture retention. A visualization of these statistics can be seen in *Figure 4*.

	10 cm	20 cm	30 cm	40 cm
Count	153.00	153.00	153.00	153.00
Mean	25.01667	30.25000	34.44902	49.23824
STD	3.72124	4.25835	5.66221	1.79976
Min	19.90000	22.95000	24.35000	46.3000
25%	21.80000	25.25000	27.40000	47.400000
50%	24.00000	31.500000	38.100000	49.050000
75%	27.750000	34.300000	38.450000	50.700000
Max	32.350000	35.400000	39.350000	53.900000

Table 1: Descriptive statistics table for probe data

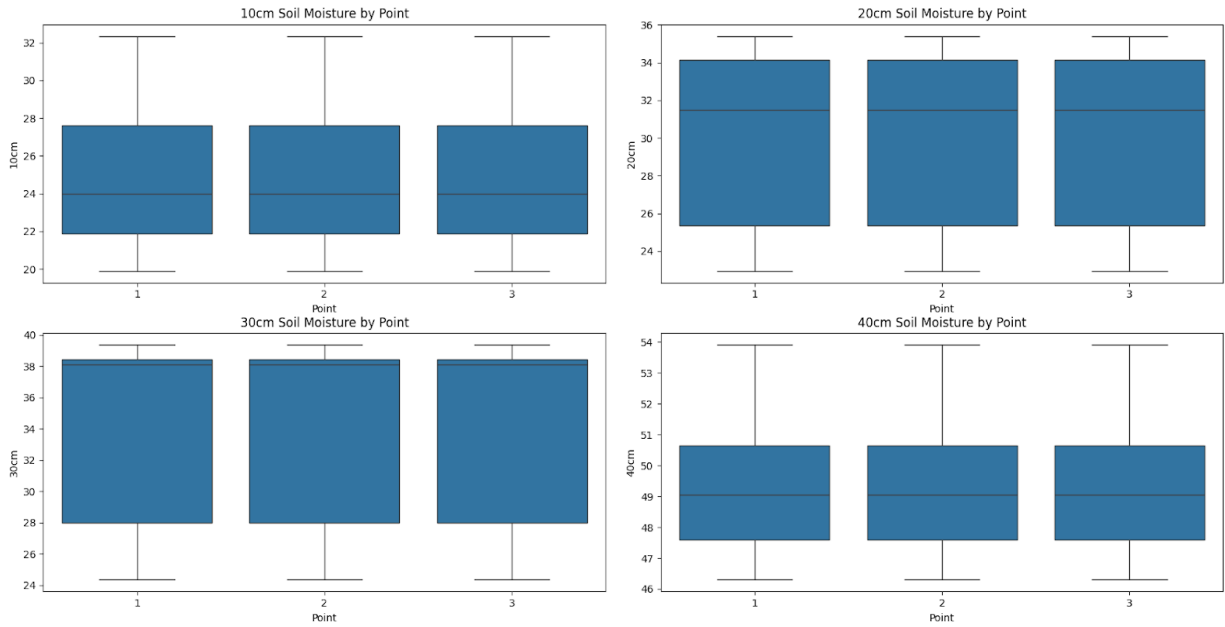


Figure 4: Box plots for probe data by depth

Correlation Analysis

The correlation matrix reveals significant relationships between moisture content at various soil depths. As seen in the heatmap below, a high correlation coefficient of 0.93 between the 20 cm and 30 cm depths indicates similar moisture retention behaviors, likely due to comparable soil textures of capillary movements within these layers as seen in *Figure 5*. Conversely, the correlation between the shallowest (10 cm) and the deepest (40 cm) depths is relatively low at 0.25, suggesting differing moisture dynamics. This disparity may be driven by factors such as surface evaporation affecting the shallower depths and more stable hydrological influences at deeper levels.

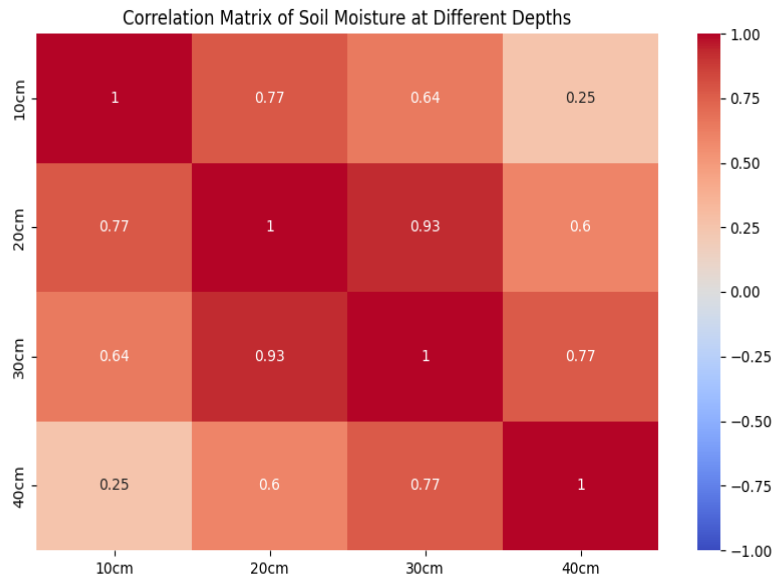


Figure 5: Correlation matrix of soil moisture at different depths

Moisture Distribution Analysis

Figure 5 shows the distribution of moisture content at each depth and further provides insights into the soil's moisture dynamics. Histograms and their corresponding fitted curves for the 10 cm depth suggest a nearly normal distribution with slight skewness towards lower moisture levels. This could show the impact of surface hydration and can possibly be linked to recent precipitation events. In contrast, the distribution at especially 30 cm displays a greater variability and a broader range of moisture content. This coupled with the higher moisture levels found at the 40 cm depth could indicate the presence of subsurface water flows or variations in soil composition that affect moisture distribution.

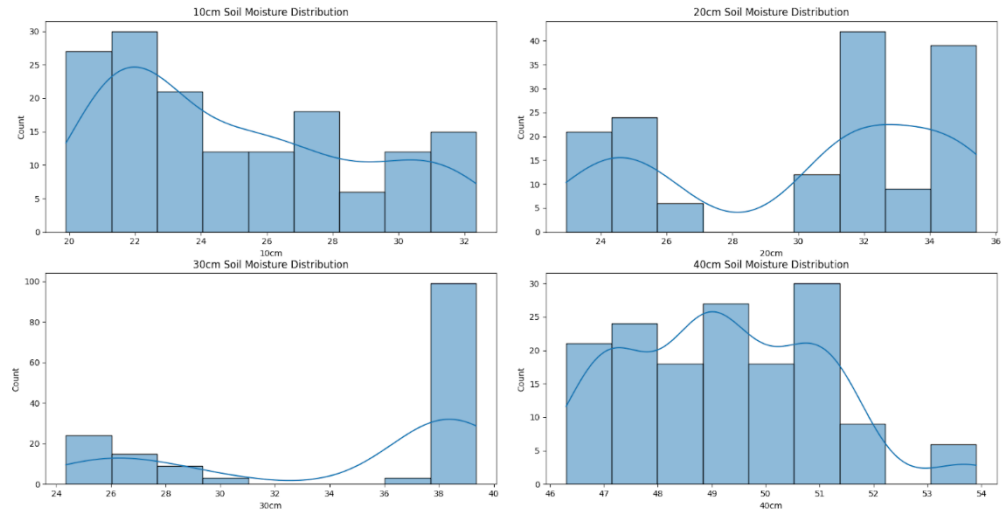


Figure 6: Distribution graph of probe data by depth

Understanding the SFCW Radar

The SFCW radar, like the AKELA AVMU, is a humble yet powerful tool for soil moisture estimation and measurement. By emitting several electromagnetic waves over a series of frequencies in a specified range, it can provide high-resolution data by stepping through frequencies and capturing important information about different materials/layers.

The data collected by the AKELA AVMU consists of data in the frequency domain. Normally, SFCW radars output data in the time domain by applying the Fast Fourier Transform (FFT) onto the vector of N (N = Number of frequency steps) complex numbers for each timestep in the frequency domain resulting in a $1 \times M$ (M = number of time steps) matrix. The AKELA AVMU applies the Inverse Fast Fourier Transform (IFFT) onto the timesteps for each frequency step resulting in a $1 \times N$ matrix [8] as seen in *Figure 7*. This is essential to understand because due to the use of the AKELA AVMU radar system, important information about depth is lost. However, the frequency domain can still be transformed into the time domain using the IFFT, but information is still lost.

The frequency domain enables detailed analysis of subsurface properties and the converted values of time domain result range bin samples. These samples provide a comprehensive view of the subsurface conditions, which is crucial for accurate soil moisture estimation.

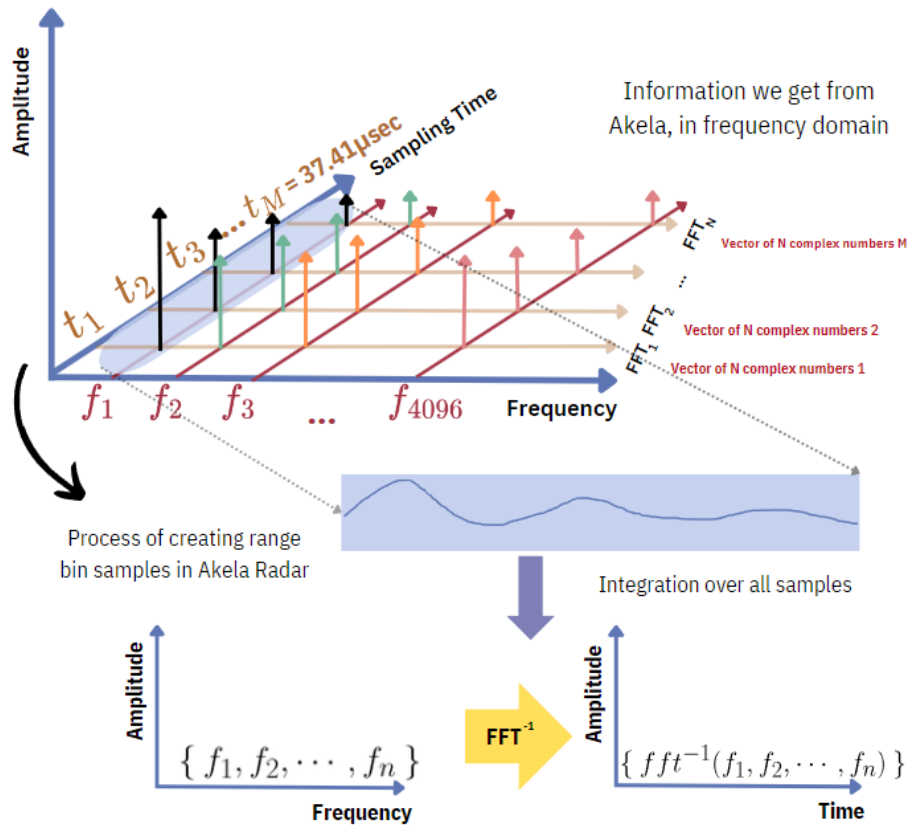


Figure 7: Image depicting how the Akela Radar creates bin samples. This is information that is received in the frequency domain which is then integrated over and an IFFT is performed to extract information in the time domain.

Dataset description

A dataset was created combining the radar data and the actual moisture values provided by the probe data. 4 steps were utilized to create this dataset. Loading radar files, running MATLAB code, reading moisture data from excel files, and combining data.

1. **Loading Radar Files:** The radar files from the Akela radar are saved in a .imb format and are stored into a folder containing all of the measurements and the excel files containing the moisture data.
2. **Running MATLAB Code:** The raw radar data in the .imb format were processed using the python MATLAB API to run a custom MATLAB script provided by our partners at MTRI. This script performs data extraction and FFT to process the data into readable complex numbers for the time and frequency domains.
3. **Reading Moisture Data:** Moisture data is read from the excel files and saved in a separate data frame. This moisture data includes measurements taken at different depths (10cm, 20cm, 30cm, 40cm) and is associated with specific days, hours, and locations (A, B, or C)
4. **Combining Data:** The processed radar data and the moisture data are then combined by matching the day, hour, and location. This process is applied to both the time and frequency domains and results in two datasets with 4104 columns and 153 rows each. Four columns of file identification, 4096 columns of complex values, and four columns of moisture data labels.

A comprehensive dataset that can be applied to machine learning models to predict soil moisture accurately is completed by processing and combining the radar and moisture data. The

enables the evaluation and comparison of different models to determine the best for soil moisture estimation using SFCW radar technology.

Machine Learning

What or how many features are important to contribute to soil moisture? Utilizing the dataset created values from 10 to 4096 both sequentially and randomly were tested to reduce the dimensionality of the data.

A variety of machine learning models were utilized and evaluated by their Root Mean Square Error (RMSE) scores. The models included: Linear Regression, Random Forest, Gradient Boost Regression, Support Vector Regressor, Multi-layer Perceptron, Extra Trees, AdaBoost, SVM with a linear kernel, Lasso and Ridge Regression, ElasticNet, and XGBoost. Each model was configured with specific parameters. For example, lasso and elastic net has 2000 iterations to ensure convergence and stability. Hyper parameter tuning was also conducted using grid search to find the best parameters for each model.

50% of the data was utilized to train the data, 20% to validate, and then 30% to test the data. Being able to easily interpret and compare performances was important and as a result, RMSE was utilized to evaluate the model performances. Test accuracy was also utilized to have a more comprehensive understanding of how accurate our models were.

Statistical analysis, mainly standard deviation, was utilized to visualize the significance of the results and the models' performances were analyzed and compared to identify best-performing models based on RMSE. Test-predictions from each model were also compared to each model and the actual values to visualize what models performed the best.

The most effective models and feature sets for accurate soil moisture estimation were able to be identified and it not only enhanced our understanding of the data but also supported the development of data- driven solutions for sustainable agriculture.

Experimental Results

This section presents the tested performance of the machine learning models in our study, where each model's effectiveness was seen using the RMSE score. After running the machine learning models a few times, a general trend can be seen.

Model	Dataset	Depth	Columns	Train RMSE	Test RMSE
XGBR	Frequency (Raw)	10 cm	50	0.0005370271564425	0.5493709537998298
XGBR	Range (Raw)	10 cm	4096	0.0002578200069026	0.8823480925267241
Gradient Boosting	Range (Raw)	20 cm	1000	3.673483290261e-05	0.4087374982253327
AdaBoost	Frequency (Raw)	20 cm	10	0.1821391096985867	0.4107473052442718
Ridge	Frequency (Magnitude)	30 cm	1000	0.0002178966045078	0.4764156459610246
Linear Regression	Frequency (Magnitude)	30 cm	1000	6.59355753730e-15	0.4766433965577863

Random Forest	Frequency (Phase)	40 cm	10	0.5250401770340998	0.5625346378224247
Linear Regression	Frequency (Magnitude)	40 cm	10	0.5805386950519528	0.5669129392924247
XGBR	Frequency (Raw)	All depths	50	0.0005279905866127	0.8141779276009659

Table 2: Best RMSEs per depth and their associated parameters

Appendix A includes graphs of the performance of each model over different numbers of columns used. Where we see the RMSE changes due to the number of columns. We can see that most models perform best with around 1000-1500 columns. Appendix B contains the best test RMSE for each model and depths.

Table 2 shows the best RMSEs per depth and their associated parameters and the lowest test RMSE score was 0.408 performed by the Gradient Boosting model at 20 cm into the ground and only using 1000 out of the 4096 range bins/columns. Other models like AdaBoost at 20 cm into the ground and Ridge Regression at 30 cm into the ground also performed well with a test RMSE score near the 0.41 range. When looking at the entire soil or at the combined 0 to 40cm range, XGBR or XGBoost Regressor performed the best utilizing the complex numbers in the frequency domain and only 50 columns.

The analysis of our models also identifies the most important features in predicting soil moisture. Models that were unable to provide these features included: Support Vector Regressor (SVR), Multi-layer Perceptron (MLP), and SVM with a non-linear kernel. Finding that the first half of the data set contained the most important features. Unfortunately, at this time, a graph

covering all the features was unable to be completed. An interesting finding was that even when the subset of columns was randomized, the first fourth of the dataset still contained the most important features. This applies to both the frequency and time domains and may not make sense since with lower frequency bandwidths, there is lower resolution.

However, from a machine learning point of view, cutting down on the number of parameters from 4096 helps each model significantly due to reduced computational complexity, leading to faster training times and less risk of overfitting. With fewer, more relevant features, each model can generalize better to the new data and improve overall performance.

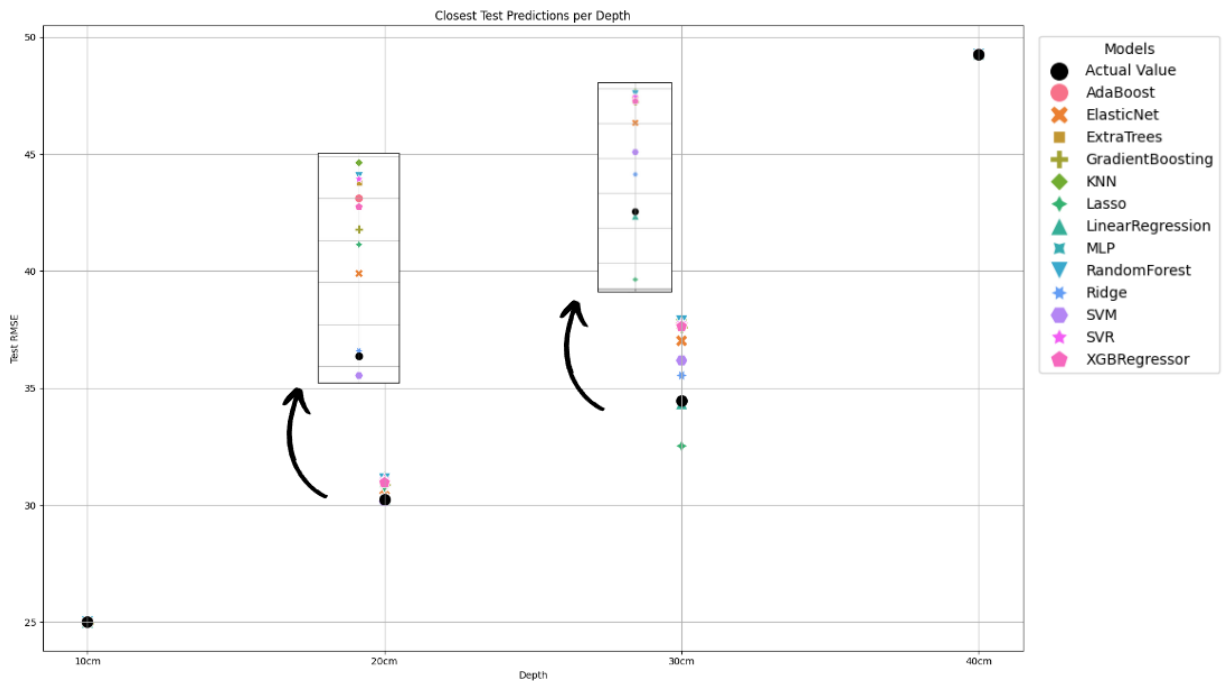


Figure 8: Graph of closest test predictions per depth for each model. Results for 20 cm and 30 cm are zoomed into.

Figure 8 shows a graph of the closest test predictions per depth for each model. As can be seen that for 10 cm and 40 cm, the models generalize and perform relatively well. However, for depths of 20 cm and 30 cm, every time the models were run, there was a small change in which

model performed the best. As the standard deviation of the actual values in 20 cm and 30 cm is larger, it is understood that the models will fluctuate as it is harder to estimate and predict.

When compared with previous studies, the results of this study perform as well or even better than previous methods. This study really highlights the dimension reduction of our data and how in previous studies the number of parameters may have affected the result.

We achieved significant improvements in model performance to estimate soil moisture by focusing on the most relevant features and reducing the dimensionality of our data. Through the integration of these techniques into agricultural management systems, globally better resource utilization, higher crop yields, and more sustainable farming practices can be achieved.

Conclusion and Future Work

With a test RMSE of 0.8141779276009659, the best performing model overall for soil moisture is XGBoost Regressor. An understanding that these transformation techniques applied to different radar signals each have their own benefits. However, when the data is converted into the time domain, using the raw complex values, and when a model is attempting to predict soil moisture for a specific depth, we see a lower RMSE and predictions that are closer to the actual value.

The findings from this study offer many practical applications in the agricultural field. By estimating soil moisture accurately using radar data and machine learning models, optimization of watering crops, reduction of water wastage, and crops receiving the ideal amount of moisture can be done. The scalability of this study is the most valuable point as the integration of radar technology and machine learning in agriculture shows the potential to be utilized in larger agricultural areas and possibly locations with various environmental conditions. This ensures that

this enhances soil moisture estimation can be used by small family farmers to large mega farms. The practicality of this technology makes it an indispensable tool to farmer's arsenal.

This study contributes to the development of non-invasive, soil moisture estimation techniques and by advancing in SFCW radar combined with machine learning algorithms, we push the boundaries of what is possible in agricultural engineering. These steps are important to developing sustainable farming practices to make informed decisions. This approach not only shows the effectiveness of soil moisture estimation but also is a model for future research where environmental and technological challenges require unique solutions.

While this model provides a robust framework for estimating soil moisture, there is a large room for improvement. Future research should focus on refining these models by integrating additional datasets, collecting more data, applying different transformations of the data for the models to make more refined choices. Experimenting with more complex neural networks like CNNs or GNNs could also possibly increase the accuracy of these predictions.

We experienced several challenges during this study, including combating the extended run times for our models as they were iterating over our data multiple times. Some models took up to two days to run on a Turing High Power Computer. This challenge posed significant hurdles in iterating through the data and refining our models. Additionally, the data collection process has been long and not as smooth as anticipated. There are chances of some collections being botched due to simple human error. Despite these obstacles, we were able to address the issue of handling complex data through our Python script, which streamlined the data preprocessing and transformation phases. Another major challenge was the limited size of our dataset. However, we were able to manage these shortcomings and achieved notable results.

The techniques in this study also have different applications beyond soil moisture estimation. They can be adapted for other estimation tasks like assessing groundwater levels, predicting drought conditions, or even estimating moisture on extraterrestrial landscapes. Expanding the applications could help address a wide range of agricultural challenges, making it more relevant on a global scale.

As we continue to push the boundary, it is important that research and development continues to focus on innovations that address agricultural challenges. This study is one example of how targeted research results in lots of benefits, and it is important we continue to support research that leads to sustainable practices.

Bibliography

[1] P. Dobriyal, A. Qureshi, R. Badola, and S. A. Hussain, “A review of the methods available for estimating soil moisture and its implications for water resource management,” *Journal of Hydrology*, vol. 458–459, pp. 110–117, Aug. 2012, doi:

<https://doi.org/10.1016/j.jhydrol.2012.06.021>.

[2] Y. Lu, W. Song, J. Lu, X. Wang, and Y. Tan, “An Examination of Soil Moisture Estimation Using Ground Penetrating Radar in Desert Steppe,” *Water*, vol. 9, no. 7, p. 521, Jul. 2017, doi:

<https://doi.org/10.3390/w9070521>.

[3] P. K. Srivastava, “Satellite Soil Moisture: Review of Theory and Applications in Water Resources,” *Water Resources Management*, vol. 31, no. 10, pp. 3161–3176, Jun. 2017, doi:

<https://doi.org/10.1007/s11269-017-1722-6>.

[4] J. Peng *et al.*, “A roadmap for highresolution satellite soil moisture applications – confronting product characteristics with user requirements,” *Remote Sensing of Environment*, vol. 252, p.

112162, 2021, doi: <https://doi.org/10.1016/j.rse.2020.112162>.

[5] K. Wu *et al.*, “A new drone-borne GPR for soil moisture mapping,” *Remote Sensing of Environment*, vol. 235, p. 111456, Dec. 2019, doi: <https://doi.org/10.1016/j.rse.2019.111456>.

[6] R. L. Carrel and University of Illinois Urbana-Champaign, *Analysis and design of the log-periodic dipole antenna*. Urbana : Electrical Engineering Research Laboratory, Engineering

Experiment Station, University of Illinois, 1961. Accessed: May 17, 2024. [Online]. Available:

<https://archive.org/details/analysisdesignof52carr/page/n5/mode/1up>

- [7] E. Gazit, “Improved design of the Vivaldi antenna,” 2022.
<https://www.semanticscholar.org/paper/Improved-design-of-the-Vivaldi-antenna-Gazit/a61271b41fa05ca33e237f754f7b1cae411fe997>
- [8] J. Taylor, “Ultra Wideband Radar Technology,” Jan. 2000, doi:
<https://doi.org/10.1201/9781420037296>.
- [9] C. M. Steelman and A. L. Endres, “Comparison of Petrophysical Relationships for Soil Moisture Estimation using GPR Ground Waves,” *Vadose Zone Journal*, vol. 10, no. 1, p. 270, 2011, doi: <https://doi.org/10.2136/vzj2010.0040>.
- [10] X. Liu, X. Dong, and D. I. Leskovar, “Ground penetrating radar for underground sensing in agriculture: a review,” *International Agrophysics*, vol. 30, no. 4, pp. 533–543, Oct. 2016, doi:
<https://doi.org/10.1515/intag-2016-0010>.
- [11] R. Wang, T. Yin, E. Zhou, and B. Qi, “What Indicative Information of a Subsurface Wetted Body Can Be Detected by a Ground-Penetrating Radar (GPR)? A Laboratory Study and Numerical Simulation,” *Remote Sensing*, vol. 14, no. 18, pp. 4456–4456, Sep. 2022, doi:
<https://doi.org/10.3390/rs14184456>.
- [12] M. Pieraccini, L. Miccinesi, and N. Rojhani, “A Doppler Range Compensation for Step-Frequency Continuous-Wave Radar for Detecting Small UAV,” *Sensors*, vol. 19, no. 6, p. 1331, Mar. 2019, doi: <https://doi.org/10.3390/s19061331>.
- [13] D. Gleich, “SAR UAV for soil moisture estimation,” in *2023 8th AsiaPacific Conference on Synthetic Aperture Radar (APSAR)*, pp. 1–4. doi:
<https://doi.org/10.1109/APSAR58496.2023.10388873>.
- [14] W. Luo, Y. H. Lee, M. L. M. Yusof, and A. C. Yucel, “A DepthAdaptive Filtering Method for Effective GPR Tree Roots Detection in Tropical Area,” *IEEE Transactions on*

Instrumentation and Measurement, vol. 72, pp. 1–10, 2023, doi:

<https://doi.org/10.1109/TIM.2023.3282654>.

[15] D. Gleich, *SAR UAV for soil moisture estimation*. 2023, pp. 1–4. doi:

<https://doi.org/10.1109/APSAR58496.2023.10388873>.

[16] W. Luo, “Advanced application of groundpenetrating radar in underground tree root systems detection and mapping,” Nanyang Technological University, 2023. doi:

<https://doi.org/10.32657/10356/170919>.

[17] W. Wagner, Vahid Naeimi, Klaus Scipal, Richard de Jeu, and José Martínez-Fernández,

“Soil moisture from operational meteorological satellites,” vol. 15, no. 1, pp. 121–131, Feb.

2007, doi: <https://doi.org/10.1007/s10040-006-0104-6>.

[18] A. Klotzsche, F. Jonard, M. C. Looms, van, and J. A. Huisman, “Measuring Soil Water

Content with Ground Penetrating Radar: A Decade of Progress,” *Vadose Zone Journal*, vol. 17,

no. 1, p. 180052, 2018, doi: <https://doi.org/10.2136/vzj2018.03.0052>.

[19] I. Nicolaescu, “Improvement of Stepped-Frequency Continuous Wave Ground-Penetrating

Radar Cross-Range Resolution,” *IEEE Transactions on Geoscience and Remote Sensing*, vol. 51,

no. 1, pp. 85–92, Jan. 2013, doi: <https://doi.org/10.1109/tgrs.2012.2198069>.

[20] Guido Tronca, Isaak Tsalicoalou, S. Lehner, and G. Catanzariti, “Comparison of pulsed and

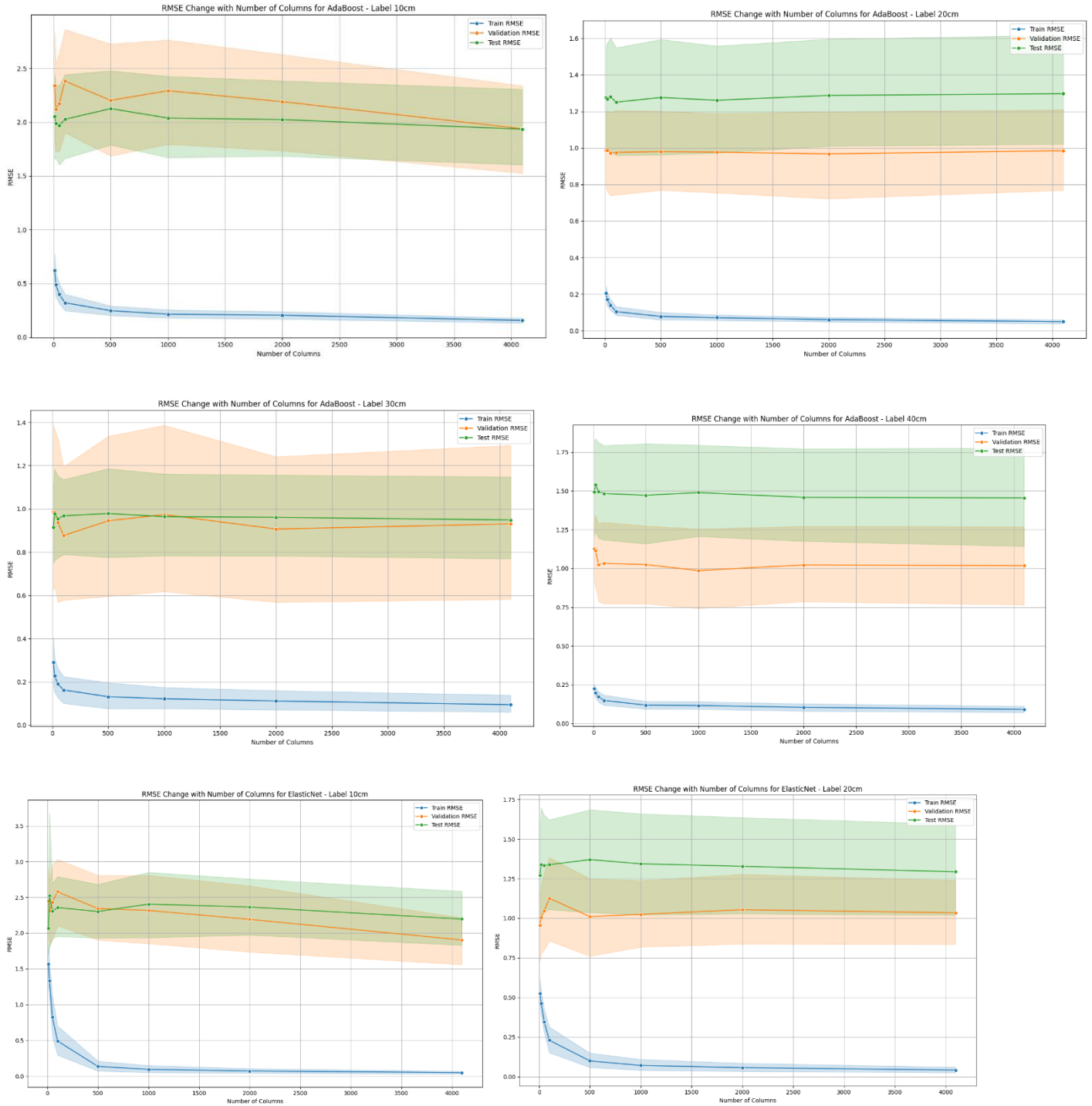
stepped frequency continuous wave (SFCW) GPR systems,” *2018 17th International Conference*

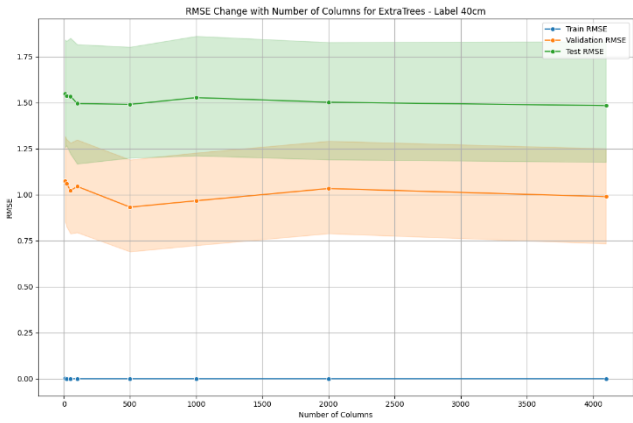
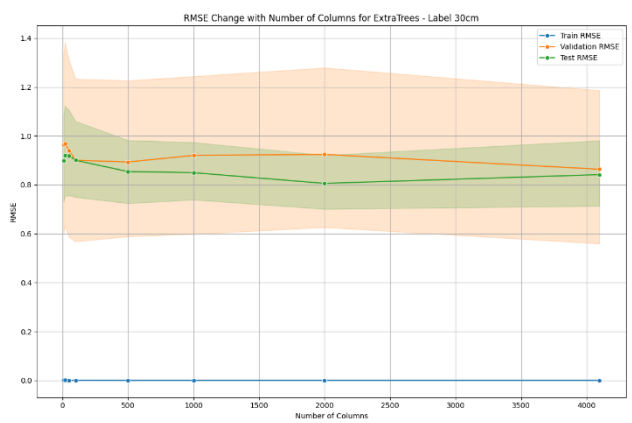
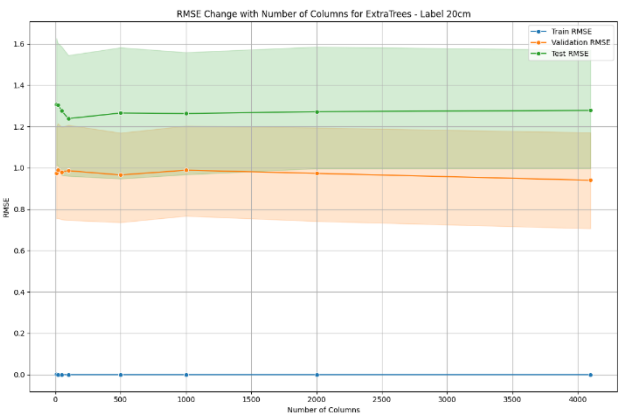
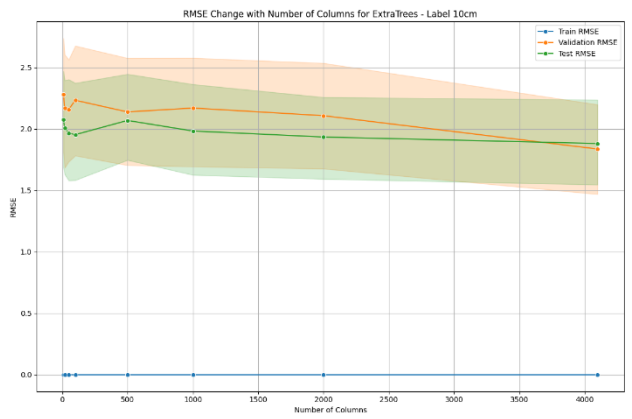
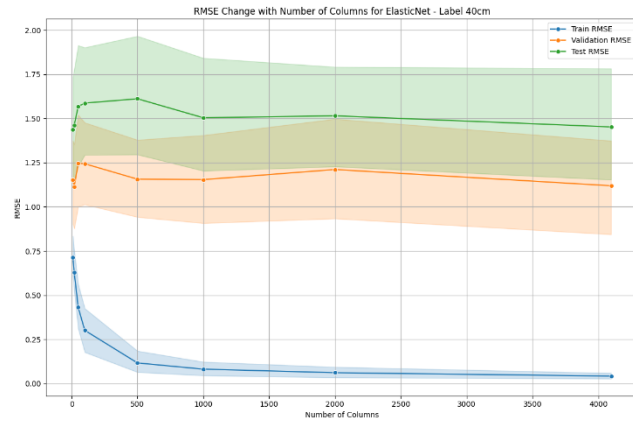
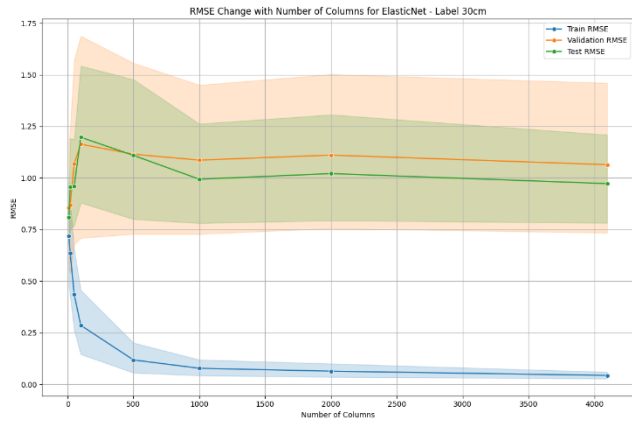
on Ground Penetrating Radar (GPR), Jun. 2018, doi:

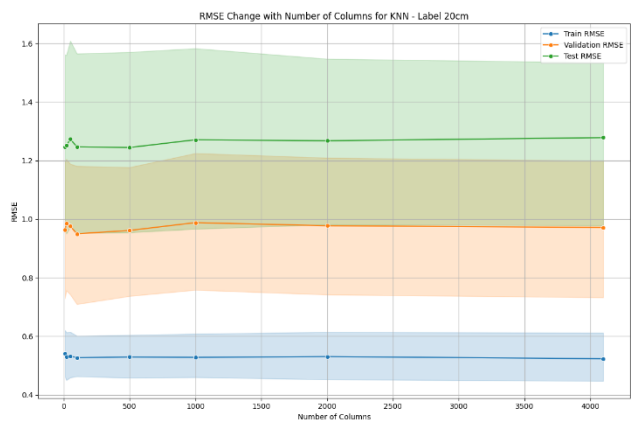
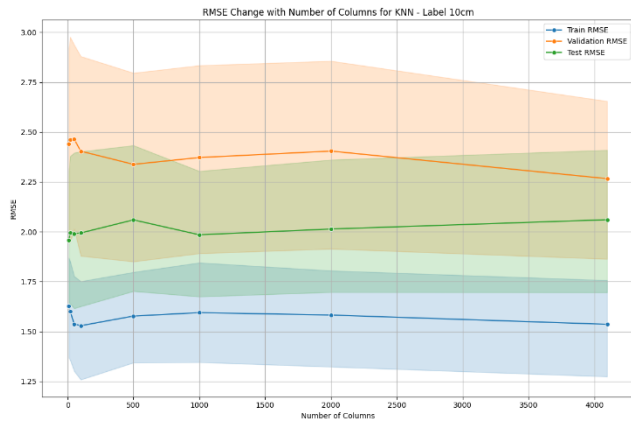
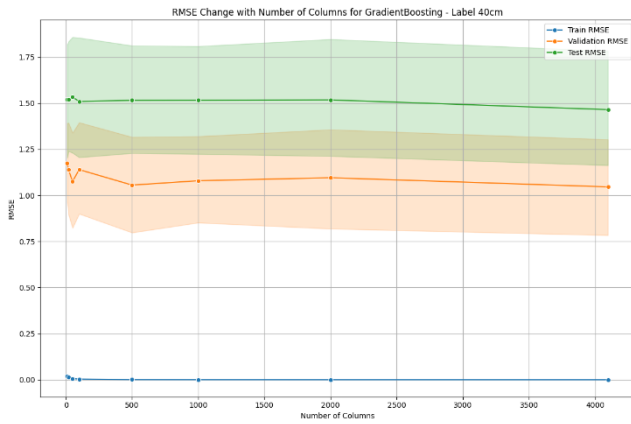
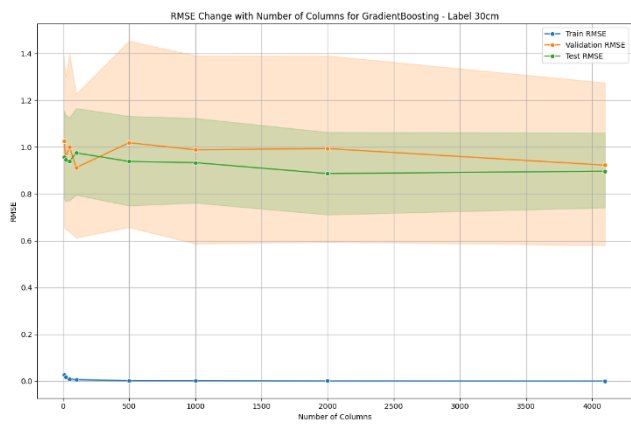
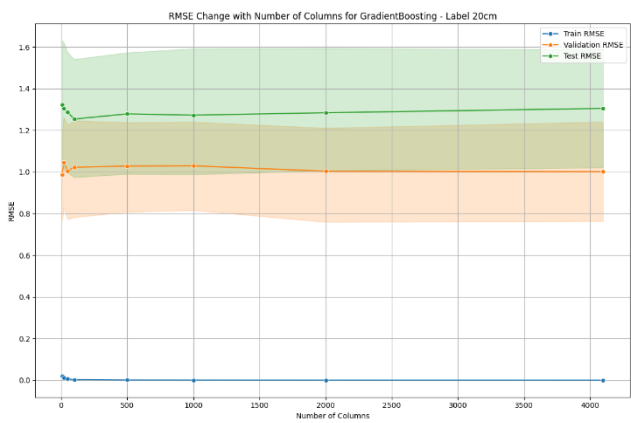
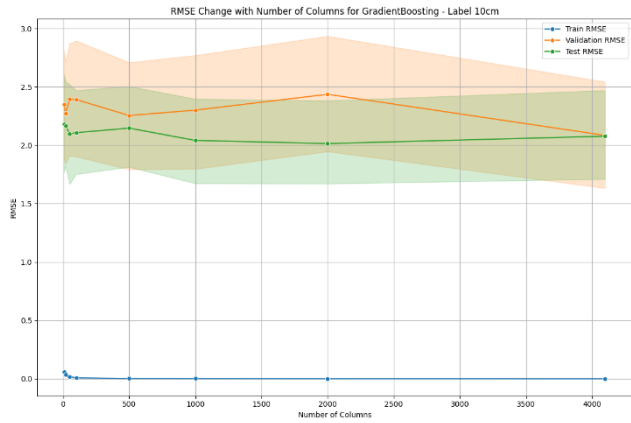
<https://doi.org/10.1109/icgpr.2018.8441654>.

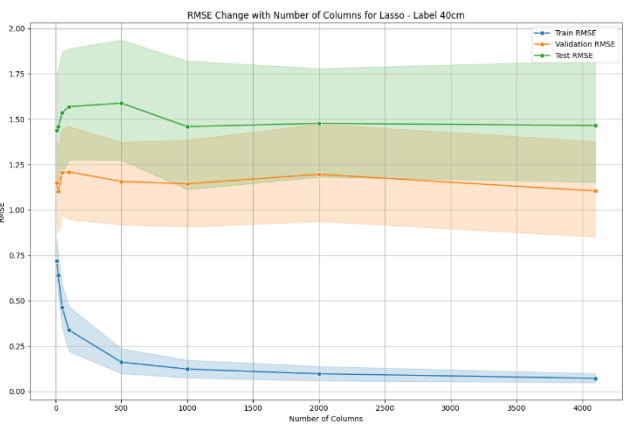
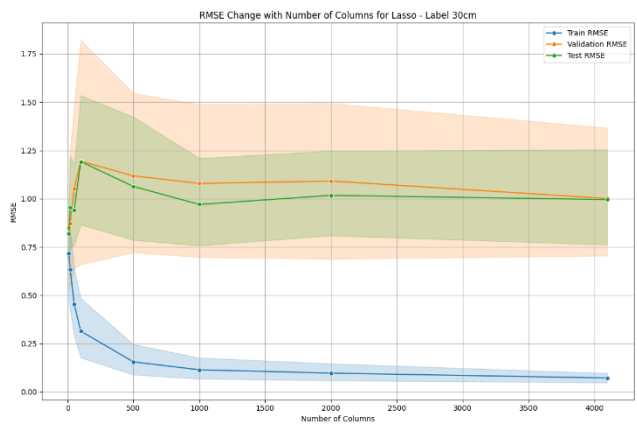
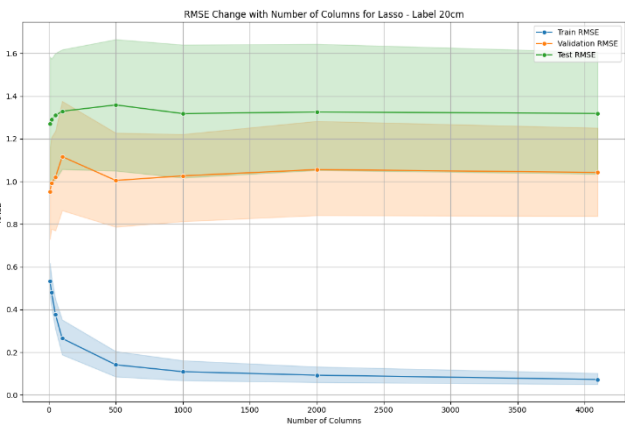
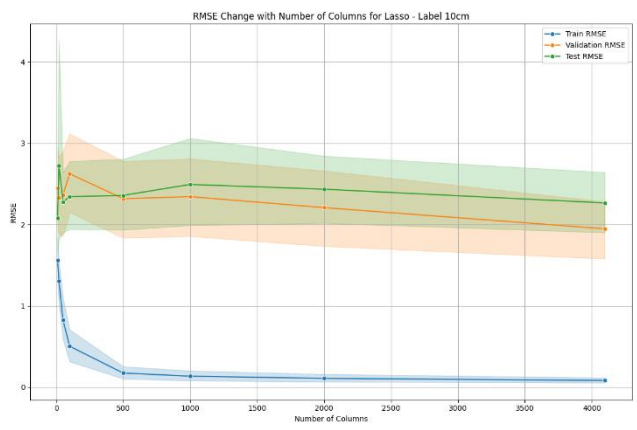
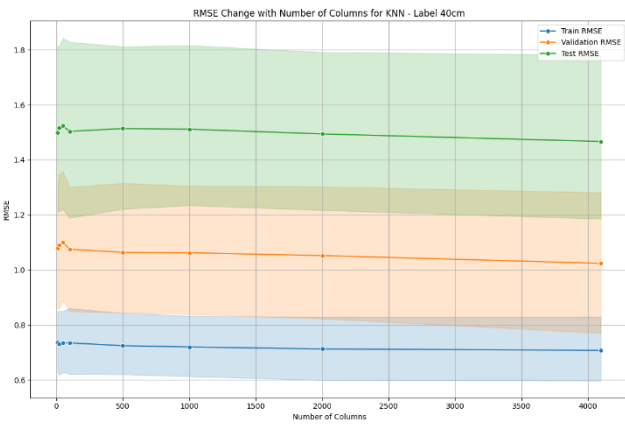
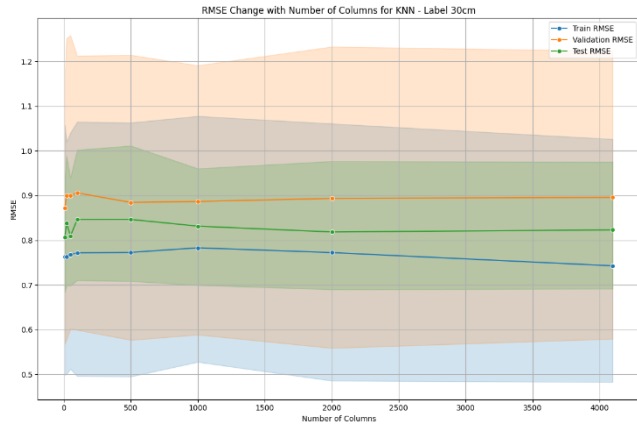
Appendix A

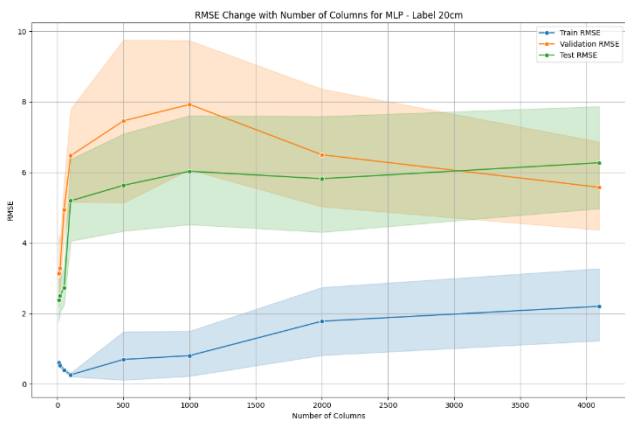
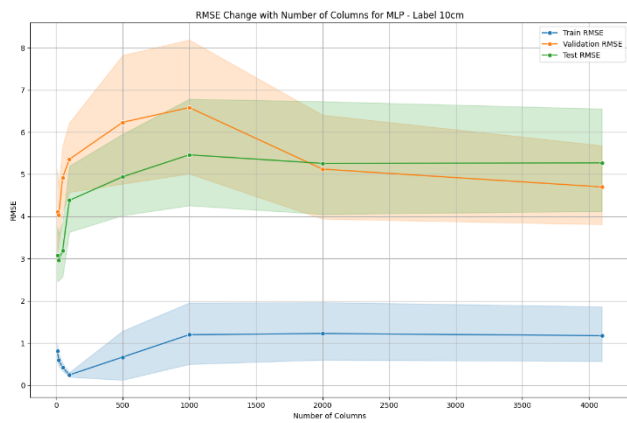
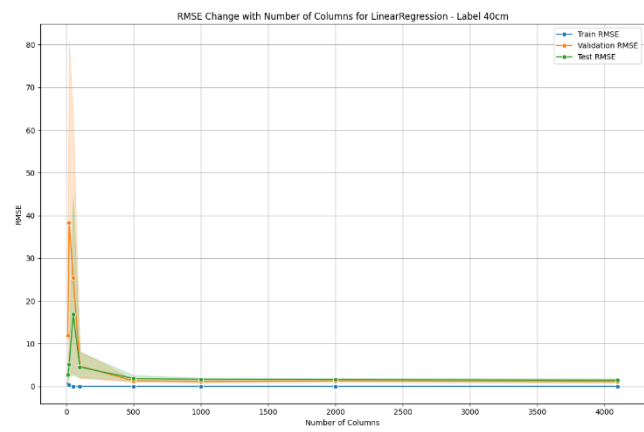
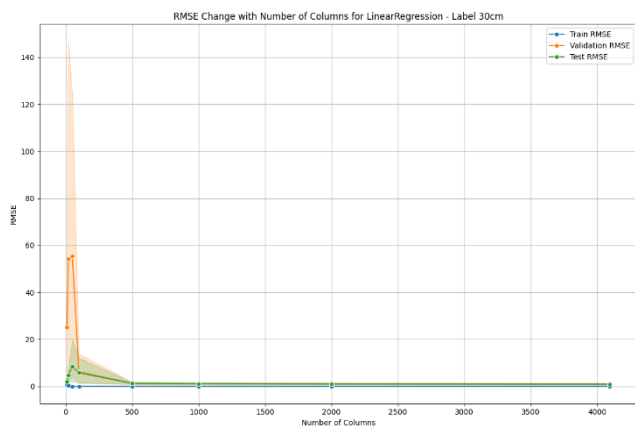
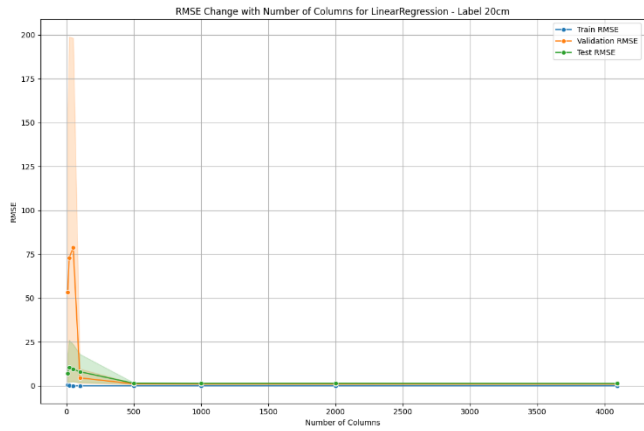
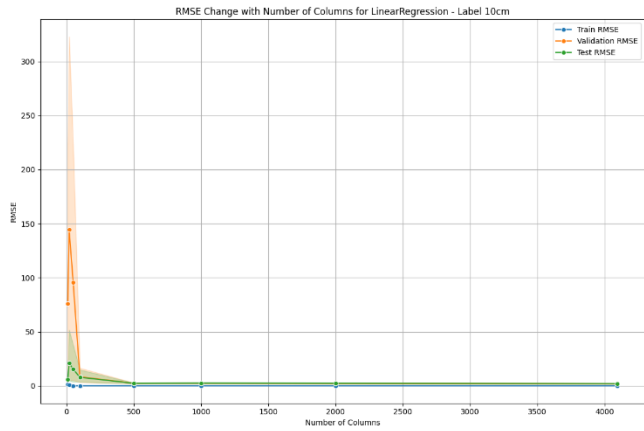
RMSE Change with different number of columns for each model.

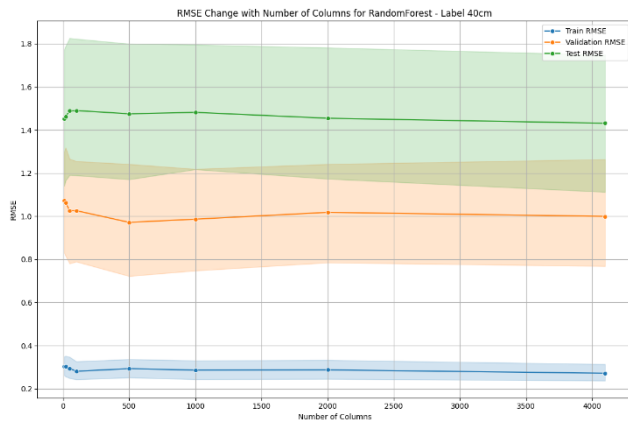
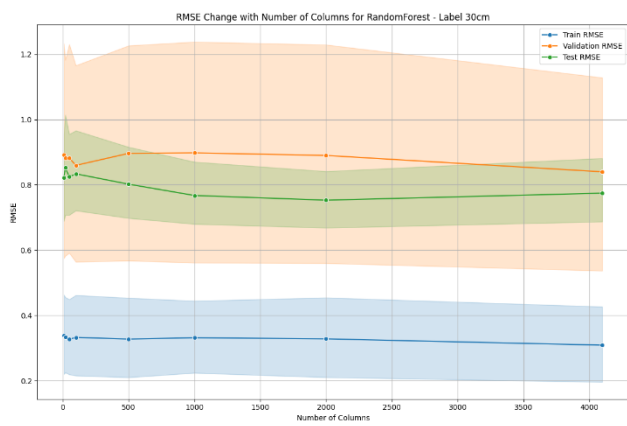
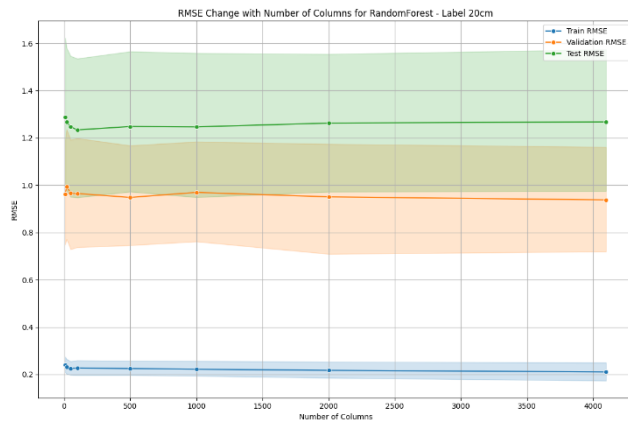
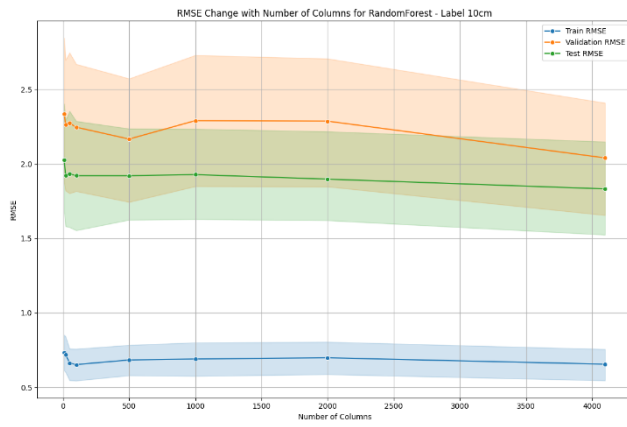
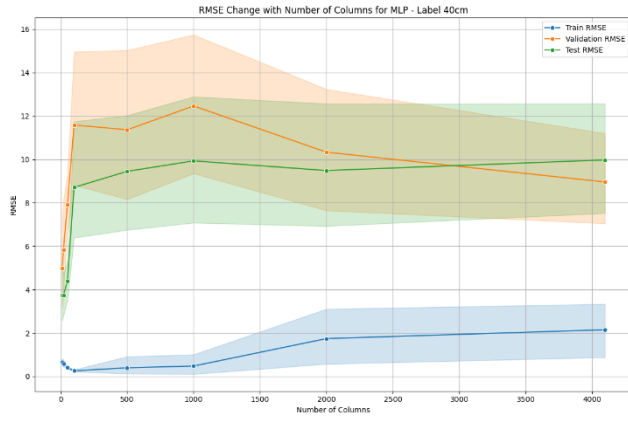
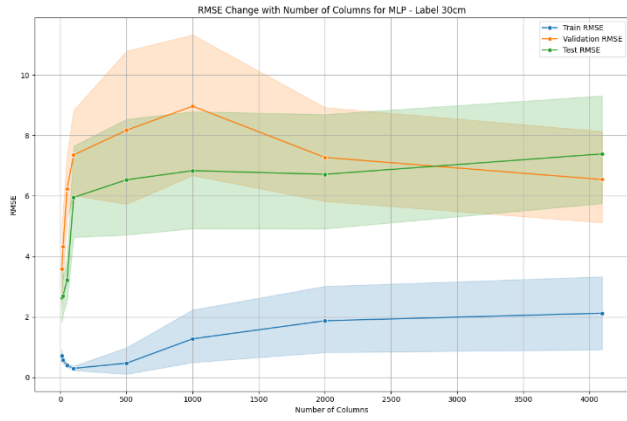


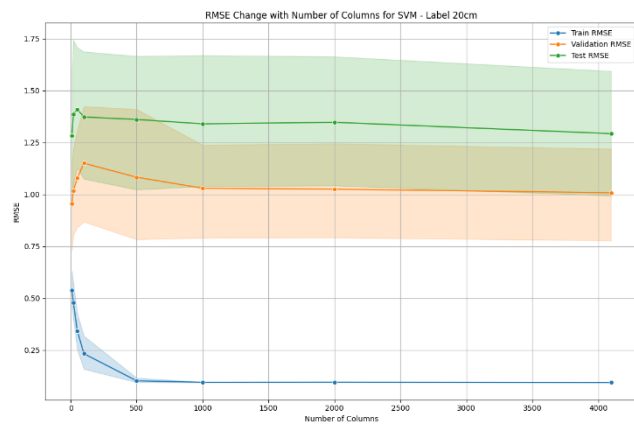
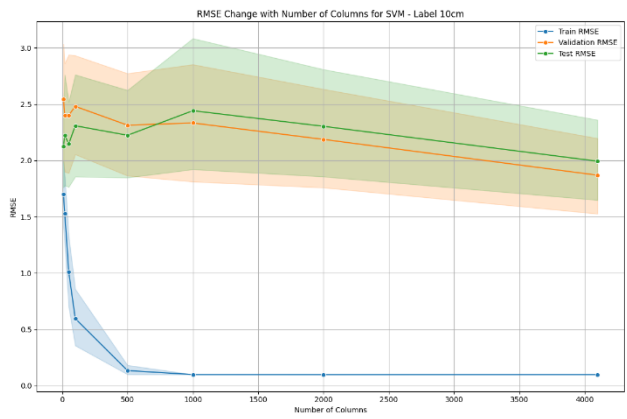
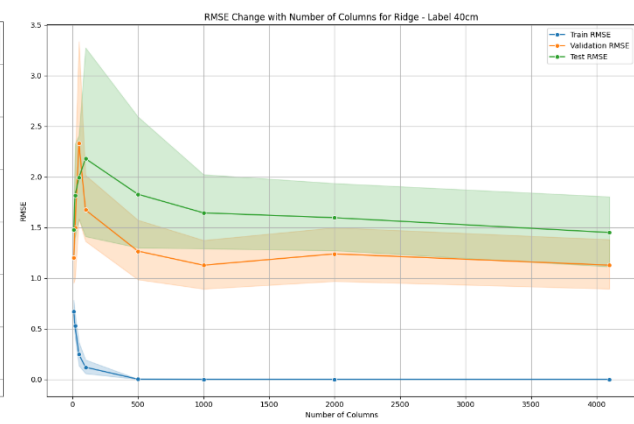
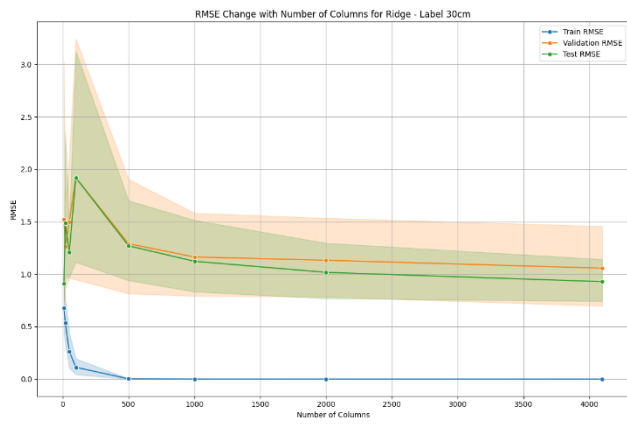
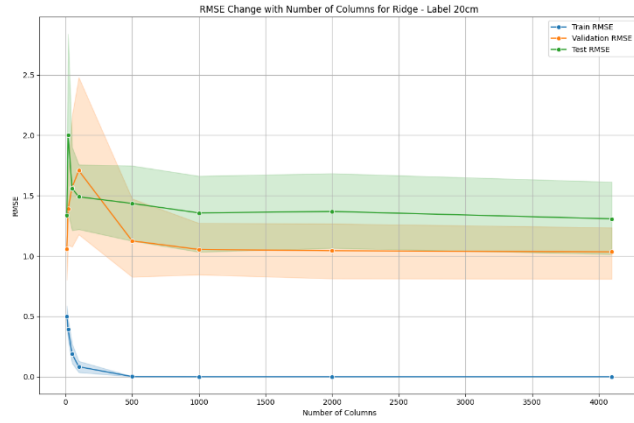
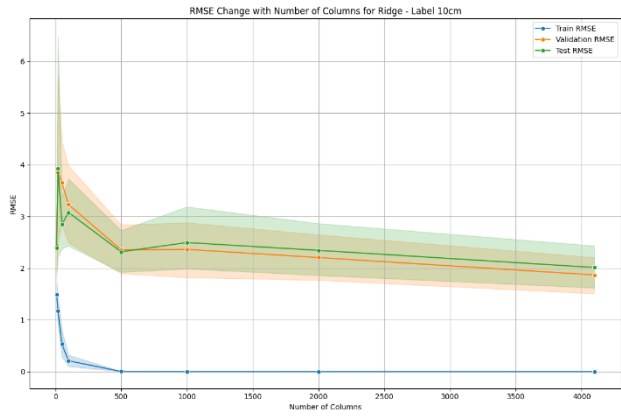


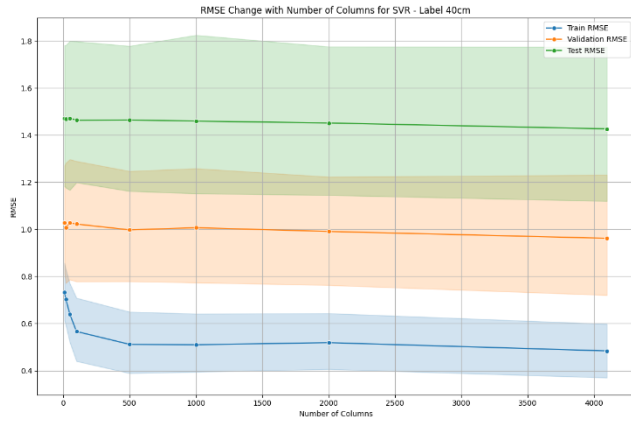
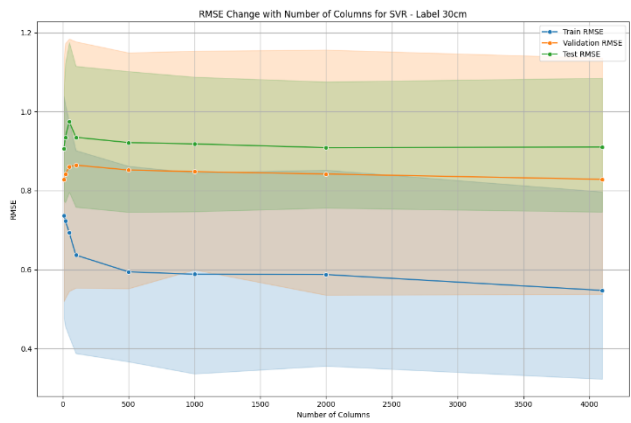
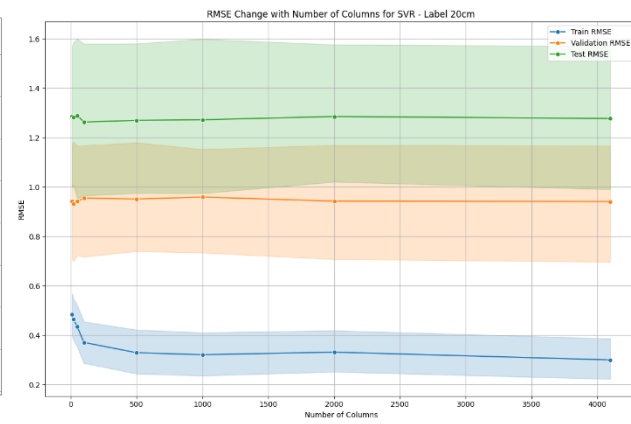
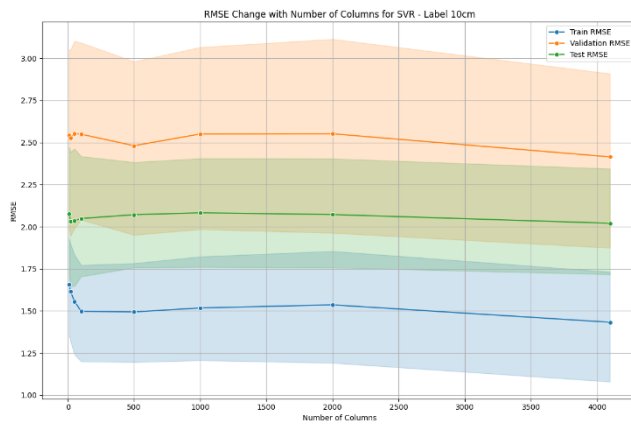
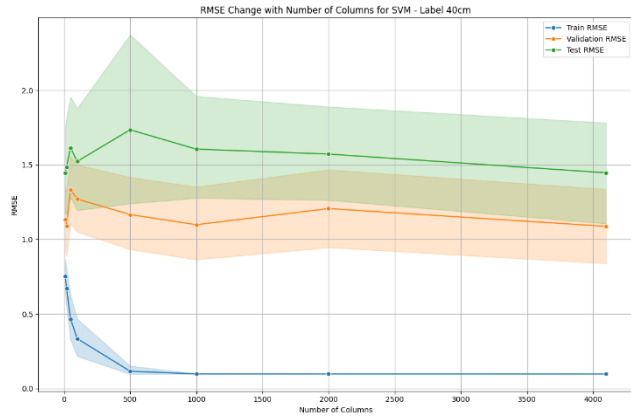
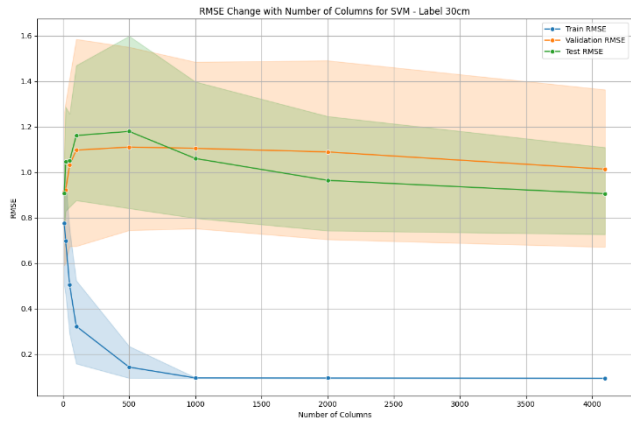


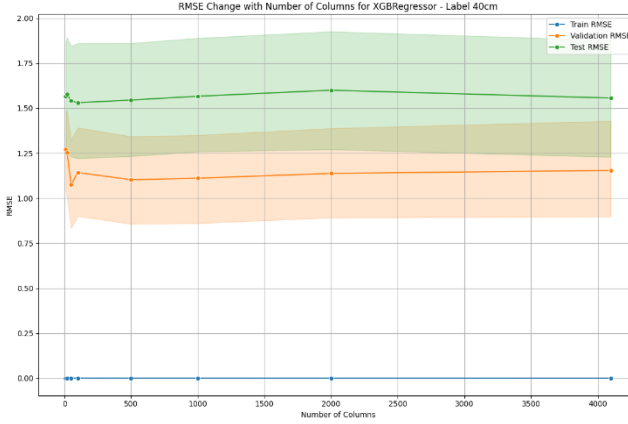
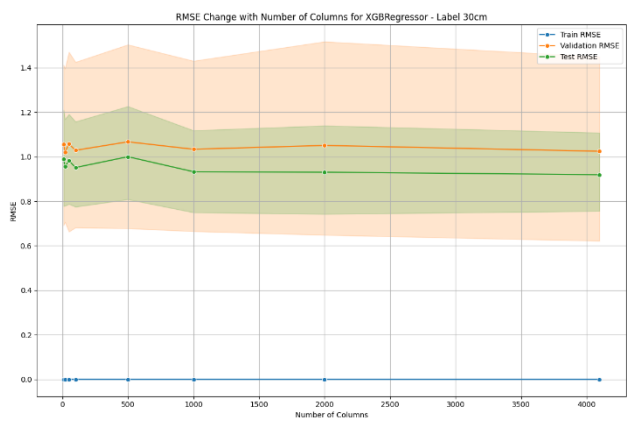
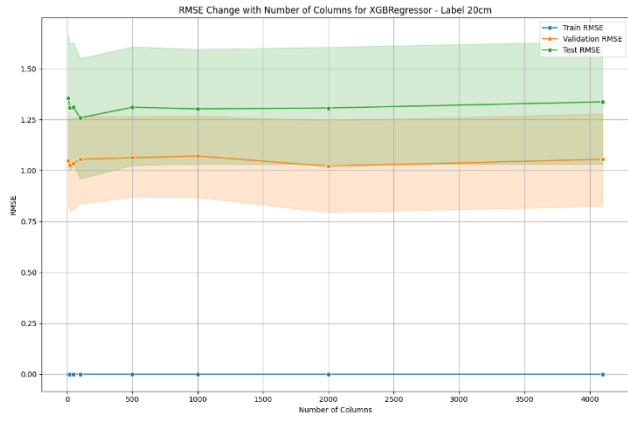
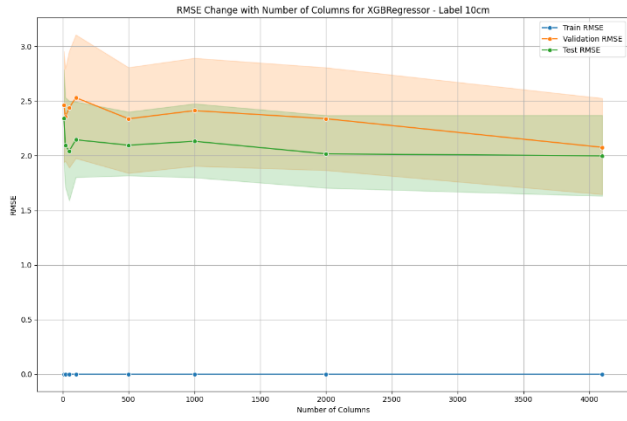












Appendix B

Best test RMSE for each model and depths.

Model	Datas et	DataT ype	Dep th	Colu mns	Ident ifier	Train RMSE	Validation RMSE	Test RMSE
LinearReg ression	Rang e	Magn itude	10c m	10	A	2.107864308 0287165	3.44185866 1426946	2.21876934 27696384
RandomF orest	Rang e	Magn itude	10c m	2000	A	0.70722	3.21534386 7691284	2.01323042 64539465
GradientB oosting	Rang e	Raw	10c m	500	A	0.000243	3.78083314 6912608	2.26379956 7459756
SVR	Frequ ency	Magn itude	10c m	20	A	2.186436039 309501	3.58606025 7619171	2.39478519 5795823
MLP	Frequ ency	Raw	10c m	20	A	0.455992518 5053935	4.48102193 7877176	2.86778463 1156147
KNN	Frequ ency	Magn itude	10c m	2000	A	2.128653069 170477	3.25375744 33260983	2.18840124 2916848
ExtraTree s	Rang e	Magn itude	10c m	4096	A	3.827305905 9653544e-14	2.24496648 77788256	2.10413015 72740005

AdaBoost	Frequ ency	Magn itude	10c m	20	A	0.760957824 1066074	3.89382712 4480495	2.33986278 58890664
SVM	Rang e	Magn itude	10c m	50	A	0.290754172 3005564	3.29127403 9215712	2.50226307 11197023
Lasso	Rang e	Raw	10c m	100	A	0.091196	3.60716727 7704664	2.33640758 4690817
Ridge	Rang e	Magn itude	10c m	10	A	2.107980647 4688096	3.44655764 2469464	2.22651974 06748527
ElasticNet	Rang e	Raw	10c m	100	A	0.066719	3.26114864 41363837	2.40391130 2631122
XGBRegr essor	Rang e	Magn itude	10c m	1000	A	0.000305	2.53945356 3178802	2.20872985 6373171
LinearReg ression	Frequ ency	Magn itude	10c m	4096	B	1.101404907 291834e-14	2.23167396 7999076	1.39350916 5354765
RandomF orest	Frequ ency	Phase	10c m	100	B	0.853823178 9037715	2.05370612 39987504	1.09379144 20720312
GradientB oosting	Frequ ency	Phase	10c m	100	B	0.026424	2.19121339 4986426	1.09202397 62946728

SVR	Frequency	Raw	10cm	50	B	2.146749626 961861	2.91275251 5096115	1.43742443 50530974
MLP	Range	Raw	10cm	50	B	0.205618276 3292285	3.07725301 47593606	1.25986092 6267239
KNN	Frequency	Phase	10cm	20	B	1.956538894 1813668	2.12301377 7628397	1.14283091 4877612
ExtraTrees	Frequency	Raw	10cm	50	B	2.862452666 6646523e-14	2.06759954 41574275	1.08490309 18704263
AdaBoost	Range	Raw	10cm	4096	B	0.142643145 6227262	2.50130513 69312285	1.09557892 29732804
SVM	Frequency	Phase	10cm	100	B	1.134963716 6908189	2.56673827 56013084	1.01596901 61348651
Lasso	Range	Raw	10cm	10	B	1.729768517 4770534	3.26529490 56454417	1.07183396 97264014
Ridge	Range	Raw	10cm	10	B	1.454802662 934575	3.13065123 6223943	1.34860971 71445373
ElasticNet	Frequency	Phase	10cm	100	B	0.989849	2.69289840 64899195	1.19833056 82358183

XGBRegressor	Frequency	Raw	10cm	50	B	0.000537	2.27976722 99171974	0.54937095 37998298
LinearRegression	Range	Raw	10cm	4096	C	8.477853123 686641e-15	0.90940861 04647998	1.13240680 1439504
RandomForest	Frequency	Raw	10cm	50	C	0.338366972 8760948	0.96210865 42069898	1.04383587 9700446
GradientBoosting	Frequency	Raw	10cm	50	C	0.008145	0.98764263 09928892	0.94253786 81205606
SVR	Frequency	Phase	10cm	20	C	0.775752627 3554938	0.88569962 51891943	1.19937526 87462953
MLP	Frequency	Phase	10cm	10	C	1.127653846 967728	4.24480001 9895871	1.09766358 94100266
KNN	Range	Phase	10cm	4096	C	0.833211657 7837022	0.99052385 13029356	1.11155859 04485643
ExtraTrees	Frequency	Raw	10cm	50	C	2.758918487 9705765e-14	1.08331450 3041465	0.98026680 04171136
AdaBoost	Frequency	Magnitude	10cm	10	C	0.450263704 4880713	1.01786643 55455174	0.96235215 35739888

SVM	Frequ ency	Raw	10c m	50	C	0.717729	0.91782543 95706492	1.06437382 54804758
Lasso	Rang e	Phase	10c m	1000	C	0.031039	1.06028189 7330974	0.944694
Ridge	Frequ ency	Raw	10c m	20	C	0.672548	0.59269871 76535463	0.94174074 43341296
ElasticNet	Rang e	Phase	10c m	1000	C	0.017253	0.99948178 46587952	1.00195102 39197642
XGBRegr essor	Rang e	Raw	10c m	4096	C	0.000258	0.60909406 22905886	0.88234809 25267241
LinearReg ression	Frequ ency	Magn itude	20c m	20	A	0.378371093 2659033	1.54057407 39824096	1.59341910 22348685
RandomF orest	Rang e	Phase	20c m	500	A	0.158757	1.51701670 64010829	2.02720709 1974077
GradientB oosting	Rang e	Phase	20c m	500	A	8.981943713 40478e-05	1.55684550 65610771	1.97086234 2997658
SVR	Rang e	Phase	20c m	2000	A	0.093536	1.49940777 96344585	2.04671936 08753083

MLP	Frequ ency	Raw	20c m	10	A	0.524258844 2330631	1.31802726 5987384	1.83110889 50933323
KNN	Rang e	Phase	20c m	1000	A	0.385846832 0172901	1.51732906 7803028	2.00016561 81426597
ExtraTree s	Rang e	Phase	20c m	4096	A	5.920005108 327088e-14	1.51654638 48824428	2.04617000 45450724
AdaBoost	Rang e	Magn itude	20c m	4096	A	0.034938	1.59961224 45536245	2.06816202 6343467
SVM	Frequ ency	Magn itude	20c m	500	A	0.096891	1.37333932 31955953	1.66526693 9313675
Lasso	Rang e	Raw	20c m	2000	A	0.037933	1.36459730 59452383	1.99952438 31321208
Ridge	Frequ ency	Magn itude	20c m	1000	A	0.000365	1.33876535 40668374	1.82103364 9856512
ElasticNet	Frequ ency	Magn itude	20c m	500	A	0.184562992 3480055	1.47351567 4439232	1.88557710 80728296
XGBRegr essor	Rang e	Phase	20c m	500	A	0.000341	1.47119712 88684276	1.85921880 2450384

LinearRegression	Frequency	Magnitude	20cm	1000	B	3.552713678 800501e-15	0.60637507 39340434	0.41378054 62133156
RandomForest	Range	Magnitude	20cm	1000	B	0.160984881 1051725	0.30174678 95438098	0.46805838 97869951
GradientBoosting	Range	Raw	20cm	1000	B	3.673483294 400261e-05	0.54710077 16569551	0.40873749 82253327
SVR	Frequency	Magnitude	20cm	500	B	0.248590370 2048383	0.43001542 43634931	0.47496
MLP	Frequency	Magnitude	20cm	10	B	0.563906298 3708821	1.16560022 18740815	0.67824776 44406166
KNN	Range	Phase	20cm	20	B	0.375310982 1645687	0.40006249 51179497	0.44401576 54858675
ExtraTrees	Frequency	Magnitude	20cm	500	B	4.320034258 3474175e-14	0.40735127 65415126	0.45615591 49567178
AdaBoost	Frequency	Raw	20cm	10	B	0.182139109 6985867	0.42621628 22228393	0.41074730 52442718
SVM	Frequency	Magnitude	20cm	1000	B	0.094353	0.47359922 37644599	0.41915966 93917491

Lasso	Frequ ency	Magn itude	20c m	500	B	0.183309372 9342521	0.48123691 10451418	0.41944534 70325814
Ridge	Frequ ency	Magn itude	20c m	1000	B	0.00017	0.60572222 55046774	0.41374244 78925561
ElasticNet	Frequ ency	Magn itude	20c m	100	B	0.342269146 7492753	0.58768497 30204745	0.45236250 78240348
XGBRegr essor	Rang e	Magn itude	20c m	1000	B	0.000311	0.36390907 12822854	0.424885
LinearReg ression	Rang e	Raw	20c m	1000	C	4.470400011 810908e-15	0.90541480 26354868	0.94641308 35201794
RandomF orest	Frequ ency	Phase	20c m	50	C	0.301066564 7143287	0.90812896 59238916	0.886293
GradientB oosting	Frequ ency	Phase	20c m	50	C	0.009744	0.99642992 58955368	0.90235606 76393608
SVR	Frequ ency	Raw	20c m	20	C	0.719827061 9770601	0.83537744 13231788	0.96053473 90276726
MLP	Frequ ency	Phase	20c m	10	C	0.829208971 9225334	2.30831363 3299861	0.90284923 82493593

KNN	Rang e	Phase	20c m	100	C	0.739432965 9347837	0.89930528 74302481	0.88546597 90189573
ExtraTree s	Frequ ency	Raw	20c m	100	C	2.990054111 9693475e-14	1.06465588 63078763	0.86815357 22439843
AdaBoost	Frequ ency	Raw	20c m	50	C	0.168782921 7076333	0.82486533 81324111	0.88456111 25248036
SVM	Rang e	Phase	20c m	20	C	0.704073223 3747752	1.26649228 44333446	0.948785
Lasso	Rang e	Raw	20c m	2000	C	0.057897	0.89931339 61171178	0.89246289 64521848
Ridge	Rang e	Raw	20c m	1000	C	2.539605874 1584068e-05	0.904029	0.94740414 38541256
ElasticNet	Frequ ency	Phase	20c m	4096	C	0.030193	0.95493583 39013084	0.88924033 55287002
XGBRegr essor	Frequ ency	Phase	20c m	100	C	0.000554	1.40562226 2579146	0.68427409 53867348
LinearReg ression	Frequ ency	Magn itude	30c m	1000	A	6.593557537 388058e-15	0.56924891 55272705	0.47664339 65577863

RandomForest	Frequency	Magnitude	30cm	20	A	0.112395877 7417378	0.39693584 17930813	0.53549483 54092638
GradientBoosting	Frequency	Magnitude	30cm	20	A	0.009132	0.43442223 56240266	0.51414954 70322257
SVR	Range	Raw	30cm	20	A	0.105702626 1819739	0.44867427 12258195	0.57895260 49252334
MLP	Frequency	Magnitude	30cm	10	A	0.471878171 8822956	0.55073882 86498257	0.71773655 45727873
KNN	Range	Magnitude	30cm	1000	A	0.226304858 2971402	0.43181303 82468781	0.57709401 31382424
ExtraTrees	Frequency	Magnitude	30cm	20	A	6.627501429 85318e-14	0.37998433 35586166	0.50786840 07693289
AdaBoost	Frequency	Magnitude	30cm	20	A	0.102915703 3876908	0.38110900 59874371	0.52743994 35796767
SVM	Frequency	Magnitude	30cm	1000	A	0.094661	0.58455571 03011868	0.52455881 39664117
Lasso	Range	Raw	30cm	2000	A	0.037313	0.48368349 35217516	0.546532

Ridge	Frequ ency	Magn itude	30c m	1000	A	0.000218	0.56920958 67616451	0.47641564 59610246
ElasticNet	Rang e	Raw	30c m	2000	A	0.020368	0.48395818 36577643	0.535805
XGBRegr essor	Frequ ency	Magn itude	30c m	20	A	0.000868	0.41008364 59413463	0.532556
LinearReg ression	Frequ ency	Raw	30c m	10	B	0.384640106 3371706	0.58537281 82240548	0.57175719 25728611
RandomF orest	Frequ ency	Phase	30c m	2000	B	0.206782931 0062887	0.36491167 59573672	0.55800176 41101109
GradientB oosting	Frequ ency	Phase	30c m	2000	B	0.000761	0.271407	0.53176663 48760874
SVR	Rang e	Phase	30c m	4096	B	0.126497660 5664468	0.38051333 22261724	0.64600736 71669917
MLP	Frequ ency	Magn itude	30c m	20	B	0.52471	1.05797243 22999302	0.65980174 72732697
KNN	Rang e	Phase	30c m	20	B	0.455170908 0725121	0.41567715 83813571	0.54190635 72241967

ExtraTrees	Range	Raw	30cm	10	B	5.673228792 5851606e-14	0.48371530 88336462	0.58393698 82530152
AdaBoost	Frequency	Phase	30cm	50	B	0.161670327 4746446	0.30679067 14976357	0.65322158 61299303
SVM	Frequency	Phase	30cm	500	B	0.093246	0.34571474 34424899	0.60449717 69069736
Lasso	Range	Raw	30cm	4096	B	0.044439	0.60610550 14911682	0.55991180 15432273
Ridge	Frequency	Raw	30cm	10	B	0.447057521 3863823	0.32042201 94549028	0.57476657 78030551
ElasticNet	Range	Raw	30cm	4096	B	0.025427	0.55623407 28340477	0.56435715 50503665
XGBRegressor	Frequency	Phase	30cm	2000	B	0.000378	0.26225257 69149622	0.51672463 53474992
LinearRegression	Frequency	Phase	30cm	10	C	1.415196046 5205755	438.142350 9575957	0.94338118 13896982
RandomForest	Frequency	Magnitude	30cm	1000	C	0.714596851 1840893	2.00935470 82956755	0.79254071 26766391

Gradient Boosting	Frequency	Phase	30cm	2000	C	0.003682	2.564081	0.987787
SVR	Range	Raw	30cm	10	C	1.499690615 500126	1.80596588 74717115	1.24794647 62552577
MLP	Frequency	Magnitude	30cm	10	C	1.681627534 5432912	1.70299182 58846923	0.94070428 86618988
KNN	Frequency	Phase	30cm	10	C	1.580638935 5081831	1.75261233 59145898	0.87222416 84337814
ExtraTrees	Frequency	Raw	30cm	2000	C	3.601232189 3809396e-14	2.14633214 75251744	0.89270568 35822188
AdaBoost	Range	Magnitude	30cm	4096	C	0.134111005 0051103	2.12536620 70240384	1.18055825 57158676
SVM	Frequency	Phase	30cm	2000	C	0.098828	2.58291210 4156752	1.00410848 49491515
Lasso	Range	Raw	30cm	10	C	1.171001109 0383643	1.84152866 70540156	0.97881939 97207092
Ridge	Frequency	Magnitude	30cm	50	C	1.299516137 1307324	1.95342172 1179948	0.82239115 15386395

ElasticNet	Rang e	Raw	30c m	10	C	1.199438832 158085	1.82727955 9386671	0.95943174 55904602
XGBRegressor	Rang e	Magn itude	30c m	4096	C	0.000261	1.90846906 26921876	0.96052939 25563978
LinearRegression	Rang e	Magn itude	40c m	10	A	0.445715224 2033577	1.91930914 85563336	1.88242186 56951663
RandomForest	Frequ ency	Magn itude	40c m	10	A	0.233669980 3616845	1.63120236 5204878	2.20386753 7988612
GradientBoosting	Frequ ency	Raw	40c m	10	A	0.019908	1.84120185 1379633	2.294456
SVR	Frequ ency	Magn itude	40c m	10	A	0.642013	1.59497234 3138777	2.24221349 36036464
MLP	Frequ ency	Magn itude	40c m	20	A	0.683902	2.02956684 4674328	1.94863328 9693175
KNN	Frequ ency	Magn itude	40c m	10	A	0.601431163 5128695	1.63287323 45163852	2.10165113 6606643
ExtraTrees	Frequ ency	Magn itude	40c m	10	A	6.177364447 876705e-14	1.57873903 40078369	2.29905559 4151643

AdaBoost	Frequ ency	Raw	40c m	20	A	0.174504	1.73208715 29171804	2.27359176 66997607
SVM	Rang e	Magn itude	40c m	10	A	0.509172758 4531212	1.74485594 6507765	2.18902548 5789448
Lasso	Frequ ency	Phase	40c m	10	A	0.604334343 2044491	1.57093305 51228462	2.205906
Ridge	Rang e	Magn itude	40c m	10	A	0.445840387 7643065	1.91442187 50643331	1.90041973 71660103
ElasticNet	Rang e	Magn itude	40c m	10	A	0.479377135 6208341	1.81176584 91092103	2.19972086 04475973
XGBRegr essor	Frequ ency	Magn itude	40c m	1000	A	0.000369	1.73337165 09510413	2.15613646 84849904
LinearReg ression	Frequ ency	Raw	40c m	4096	B	1.632359285 0267968e-14	1.59454550 55677131	0.62642502 62540167
RandomF orest	Frequ ency	Phase	40c m	10	B	0.525040177 0340998	0.77595147 23872939	0.56253463 78224247
GradientB oosting	Frequ ency	Phase	40c m	20	B	0.05938	0.82829207 26352428	0.58940442 43176602

SVR	Rang e	Raw	40c m	100	B	0.828399315 9775306	0.79868103 13677444	1.05985362 57903295
MLP	Frequ ency	Phase	40c m	10	B	1.262579634 668867	1.43816765 9888509	0.81376
KNN	Rang e	Raw	40c m	100	B	1.042519650 7607035	0.80703934 22875971	0.86832453 61038703
ExtraTree s	Rang e	Phase	40c m	100	B	5.384051330 5986836e-14	0.76836510 68990552	0.99367450 97113018
AdaBoost	Rang e	Phase	40c m	100	B	0.187758512 6791617	0.51637968 13741183	1.01894880 3737354
SVM	Frequ ency	Raw	40c m	4096	B	0.097979	1.46462466 03175772	0.68308925 40768214
Lasso	Frequ ency	Raw	40c m	4096	B	0.184638871 3949585	1.31742106 9226213	0.68268273 41480048
Ridge	Frequ ency	Raw	40c m	4096	B	6.383118119 147653e-05	1.59445316 48221385	0.62645361 64969675
ElasticNet	Frequ ency	Raw	40c m	4096	B	0.110063802 6756353	1.48982534 69663705	0.64710721 81601092

XGBRegressor	Frequency	Phase	40cm	100	B	0.000562	1.07361764 10252318	1.05508805 74283052
LinearRegression	Frequency	Magnitude	40cm	10	C	0.580538695 0519528	0.59867572 29586451	0.56691293 92924247
RandomForest	Range	Phase	40cm	10	C	0.291993305 1934369	0.53992048 02561152	0.70199463 58413245
GradientBoosting	Range	Phase	40cm	10	C	0.014683	0.64267454 16430137	0.63690758 00351799
SVR	Frequency	Magnitude	40cm	4096	C	0.366481558 2387216	0.39106014 64390477	0.74114260 55306967
MLP	Frequency	Phase	40cm	10	C	1.147735682 2983458	5.51990709 4243267	0.96796006 39560508
KNN	Range	Magnitude	40cm	2000	C	0.602916522 6906085	0.55223409 89109621	0.79047454 10195102
ExtraTrees	Frequency	Magnitude	40cm	4096	C	6.766756459 892375e-14	0.45043870 97597289	0.63230619 56045962
AdaBoost	Range	Phase	40cm	10	C	0.213857587 6770671	0.55427882 75500713	0.63460665 34973941

SVM	Frequ ency	Phase	40c m	1000	C	0.0989	0.50648597 23575672	0.65208457 19682261
Lasso	Frequ ency	Phase	40c m	1000	C	0.071252	0.75172134 94132432	0.60753372 45457948
Ridge	Rang e	Magn itude	40c m	100	C	0.000637	0.816214	0.60039104 40111043
ElasticNet	Rang e	Raw	40c m	20	C	0.316218725 8558846	0.25484910 36490274	0.62221913 23272201
XGBRegr essor	Rang e	Phase	40c m	100	C	0.000381	0.38208900 18373016	0.58056226 96748597
LinearReg ression	Rang e	Magn itude	All Dep ths	10	A	1.096641896 9789136	2.11691690 83021546	1.90196852 86727608
RandomF orest	Rang e	Magn itude	All Dep ths	500	A	0.400597281 9324575	1.60995959 28547323	1.90168375 84591857
GradientB oosting	Rang e	Magn itude	All Dep ths	2000	A	0.000116	2.19206315 5483339	1.98897251 9845402

SVR	Frequ ency	Magn itude	All Dep ths	20	A	1.151971964 8834206	2.11143646 21721635	1.99662076 5059247
MLP	Frequ ency	Magn itude	All Dep ths	10	A	1.095905854 187924	2.17265076 6221704	2.34171949 9358615
KNN	Frequ ency	Magn itude	All Dep ths	2000	A	1.121327338 469905	2.00830074 31657243	1.93062732 68033896
ExtraTree s	Rang e	Magn itude	All Dep ths	1000	A	5.739737313 350087e-14	1.55737902 06826577	1.96056041 4938789
AdaBoost	Rang e	Magn itude	All Dep ths	2000	A	0.109742112 4542717	1.73344351 87238233	1.99725486 85839056
SVM	Rang e	Magn itude	All Dep ths	50	A	0.166834	2.02221879 09579774	2.07895611 40906416

Lasso	Frequ ency	Phase	All Dep ths	10	A	1.047965109 806155	1.86228050 83457084	1.98775683 12181528
Ridge	Rang e	Magn itude	All Dep ths	10	A	1.096712549 689246	2.11771733 0144321	1.90759963 95494863
ElasticNet	Frequ ency	Phase	All Dep ths	10	A	1.046954001 0821945	1.86535137 41296268	1.987495
XGBRegr essor	Rang e	Magn itude	All Dep ths	1000	A	0.000299	1.79509298 94490508	1.99111275 42788016
LinearReg ression	Frequ ency	Magn itude	All Dep ths	4096	B	7.799355160 121197e-15	1.46733402 28997305	0.90719362 59224798
RandomF orest	Frequ ency	Phase	All Dep ths	50	B	0.528527967 5665243	1.12206004 39314743	0.86334172 24294822

GradientBoosting	Frequency	Phase	All Depths	100	B	0.016143	1.22560228 30569413	0.84916595 39570483
SVR	Frequency	Raw	All Depths	50	B	1.253184651 2599332	1.54145573 2673341	1.02848427 29670478
MLP	Frequency	Magnitude	All Depths	10	B	0.961276	2.18308545 6319924	1.30922084 41515976
KNN	Frequency	Phase	All Depths	20	B	1.174683172 4152498	1.26942777 4629183	0.84503513 24057479
ExtraTrees	Frequency	Phase	All Depths	100	B	0.001532	0.98028126 14563704	0.89337947 73918865
AdaBoost	Frequency	Phase	All Depths	4096	B	0.143336905 0372465	1.12153682 74893007	0.89195419 34649378

SVM	Frequ ency	Magn itude	All Dep ths	4096	B	0.096824	1.38909050 2015466	0.91225336 13398404
Lasso	Frequ ency	Raw	All Dep ths	10	B	1.212836271 6991623	1.32039349 6695868	0.947461
Ridge	Frequ ency	Magn itude	All Dep ths	4096	B	4.794470820 201292e-05	1.46728809 73245186	0.90716857 74954706
ElasticNet	Frequ ency	Raw	All Dep ths	10	B	1.210772589 3222607	1.32543447 0368175	0.94038667 20350724
XGBRegr essor	Frequ ency	Raw	All Dep ths	50	B	0.000528	1.27774592 53123535	0.81417792 76009659
LinearReg ression	Frequ ency	Phase	All Dep ths	1000	C	6.045705523 364516e-15	1.44069770 8486255	1.04947614 47791523

RandomForest	Frequency	Magnitude	All Depths	2000	C	0.455183998 2053648	1.20355738 0097643	0.999281
GradientBoosting	Frequency	Magnitude	All Depths	4096	C	0.000913	1.13818206 04991737	1.02636040 12717662
SVR	Frequency	Phase	All Depths	20	C	0.981863155 0494034	1.11917518 28498022	1.10955341 39397634
MLP	Frequency	Phase	All Depths	10	C	1.078745922 3363216	1.80999258 5717141	1.09127455 07838817
KNN	Frequency	Phase	All Depths	10	C	1.037482262 2312363	1.18584226 39626227	0.97266065 51105074
ExtraTrees	Frequency	Phase	All Depths	2000	C	4.339064446 5454556e-14	1.37397191 9632095	1.05084741 84556875

AdaBoost	Frequ ency	Phase	All Dep ths	10	C	0.532385072 9572529	1.46034010 2100942	1.09408074 56154686
SVM	Frequ ency	Phase	All Dep ths	1000	C	0.099514	1.42680324 43735466	1.04294717 13856593
Lasso	Frequ ency	Phase	All Dep ths	20	C	0.894852	1.25759638 03847243	1.00159956 03771926
Ridge	Frequ ency	Phase	All Dep ths	20	C	0.840529155 7038305	4.07603780 7313566	0.99607387 03352212
ElasticNet	Frequ ency	Phase	All Dep ths	20	C	0.891541	1.35903093 69221352	1.00030510 19616456
XGBRegr essor	Rang e	Magn itude	All Dep ths	4096	C	0.000282	1.23268225 72673526	1.05929839 26121602